USGS
science for a changing world

Prepared in cooperation with Rice Creek Watershed District

Sediment Monitoring and Streamflow Modeling Before and After a Stream Restoration in Rice Creek, Minnesota, 2010–2019

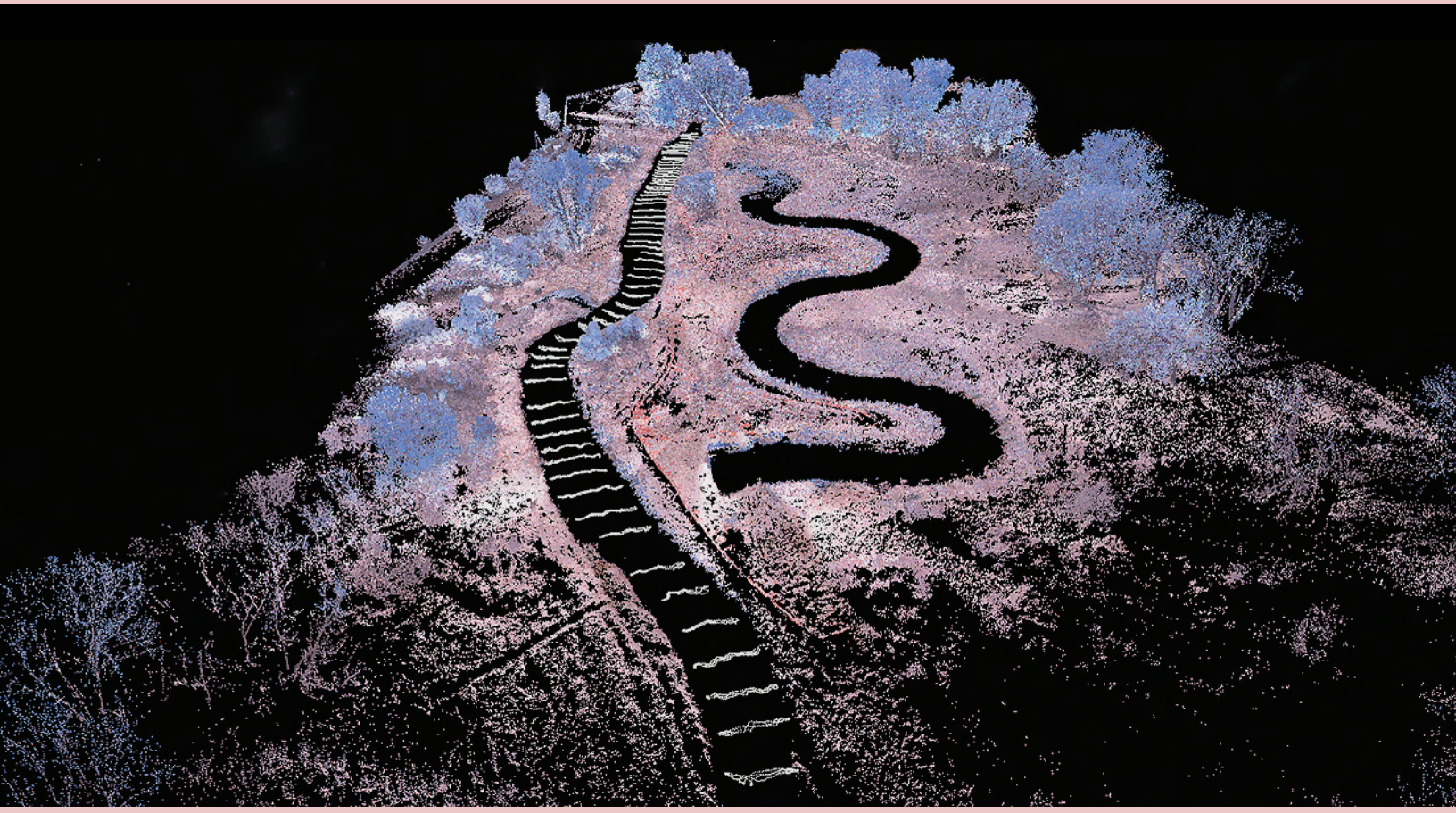

Scientific Investigations Report 2022–5004

U.S. Department of the Interior
U.S. Geological Survey

Sediment Monitoring and Streamflow Modeling Before and After a Stream Restoration in Rice Creek, Minnesota, 2010–2019

By Joel T. Groten, Colin T. Livdahl, Stephen B. DeLong, J. William Lund, Jonathan M. Nelson, Erin N. Coenen, Jeffrey R. Ziegeweid, and Matthew J. Kocian

Prepared in cooperation with Rice Creek Watershed District

Scientific Investigations Report 2022–5004

U.S. Geological Survey, Reston, Virginia: 2022

For more information on the USGS—the Federal source for science about the Earth, its natural and living resources, natural hazards, and the environment—visit https://www.usgs.gov or call 1–888–ASK–USGS.

For an overview of USGS information products, including maps, imagery, and publications, visit https://store.usgs.gov/.

Suggested citation:
Groten, J.T., Livdahl, C.T., DeLong, S.B., Lund, J.W., Nelson, J.M., Coenen, E.N., Ziegeweid, J.R., and Kocian, M.J., 2022, Sediment monitoring and streamflow modeling before and after a stream restoration in Rice Creek, Minnesota, 2010–2019: U.S. Geological Survey Scientific Investigations Report 2022–5004, 40 p., https://doi.org/10.3133/sir20225004.

Data associated with this report,
Groten, J.T., Livdahl, C.T., and DeLong, S.B., 2022, Suspended sediment and bedload data, simple linear regression models, loads, elevation data, and FaSTMECH models for Rice Creek, Minnesota, 2010-2019: U.S. Geological Survey data release, https://doi.org/10.5066/P9SJIY32.

U.S. Geological Survey, 2021c, USGS water data for the Nation: U.S. Geological Survey National Water Information System database, accessed February 5, 2021, at https://doi.org/10.5066/F7P55KJN.

ISSN 2328-0328 (online)

Acknowledgments

This report presents a compilation of information, resources, and expertise supplied by many individuals. The authors would like to thank the Rice Creek Watershed District for their assistance with this study.

Christopher Ellison, Sara Levin, Jerry Storey, Brett Savage, Julia Prokopec, Sara Levin, Patrick Farrell, Erich Kessler, and Zachary Engle of the U.S. Geological Survey and Brent Mason, Joshua Ayers, and Kristen Kieta formerly with the U.S. Geological Survey are acknowledged for assistance with field sampling, project planning, surveying, data analyses, and data management. Anna Baker and Paul Kinzel of the U.S. Geological Survey are acknowledged for their technical reviews of the report.

Contents

Figures

Tables

Conversion Factors

U.S. customary units to International System of Units

Multiply	By	To obtain
	Volume	
pint (pt)	0.4732	liter (L)
quart (qt)	0.9464	liter (L)

Multiply	By	To obtain
	Flow rate	
cubic foot per second (ft^3/s)	0.02832	cubic meter per second (m^3/s)
	Mass	
ton, short (2,000 lb)	0.9072	metric ton (t)

International System of Units to U.S. customary units

Multiply	By	To obtain
	Length	
millimeter (mm)	0.03937	inch (in.)
meter (m)	3.281	foot (ft)
kilometer (km)	0.6214	mile (mi)
	Area	
square kilometer (km^2)	247.1	acre
	Volume	
liter (L)	33.81402	ounce, fluid (fl. oz)
	Flow rate	
meter per second (m/s)	3.281	foot per second (ft/s)
cubic meter per second (m^3/s)	35.31	cubic foot per second (ft^3/s)
	Mass	
milligram (mg)	0.0003527	ounce, avoirdupois (oz)
metric ton (t)	1.102	ton, short [2,000 lb]

Datum

Vertical coordinate information is referenced to the North American Vertical Datum of 1988 (NAVD 88).

Horizontal coordinate information is referenced to the North American Datum of 1983 (NAD 83).

Supplemental Information

Concentrations of physical constituents in water are given in milligrams per liter (mg/L).

Water year (WY) is the 12-month period, October 1 through September 30, and is designated by the calendar year in which it ends.

Abbreviations

BL	bedload transport
EWI	equal-width increment
GH	gage height
GNSS	global navigation satellite system
GSE	ground surface elevation
iRIC	International River Interface Cooperative
LEV	lateral eddy velocity
MRCRP	Middle Rice Creek Restoration Project
RCWD	Rice Creek Watershed District
RMSE	root-mean-square error
RTK	real time kinematic
SSC	suspended-sediment concentration
SLR	simple linear regression
SSL	suspended-sediment load
USGS	U.S. Geological Survey
WSE	water surface elevation
WY	water year

Sediment Monitoring and Streamflow Modeling Before and After a Stream Restoration in Rice Creek, Minnesota, 2010–2019

By Joel T. Groten,[1] Colin T. Livdahl[1], Stephen B. DeLong[1], J. William Lund[1], Jonathan M. Nelson[1], Erin N. Coenen[1], Jeffrey R. Ziegeweid[1], and Matthew J. Kocian[2]

Abstract

The Rice Creek Watershed District (RCWD) cooperated with the U.S. Geological Survey to establish a 10-year suspended sediment and bedload monitoring and streamflow modeling study to evaluate the effects of two restored meander sections on middle Rice Creek in Arden Hills, Minnesota. The RCWD goals of this stream restoration were to reduce water quality impairments, improve aquatic habitat, and reduce associated costs of dredging a sedimentation pond. During the study there were several factors that introduced uncertainty in the sampling results; however, the sampling results indicated there was an increase in the post-stream restoration sediment data because of higher streamflows during the post-stream than the pre-stream restoration monitoring period. The negative relation between suspended fines and streamflow was explained by a reduction in the supply of fines with increasing streamflows. The positive relation among suspended sand, bedload, and streamflow was because of those constituents having a functional relation with the hydraulic properties of flow and a consistent supply of sand. Two-dimensional flow modeling simulations indicated the downstream restored section had less shear stress, more pools, and could access the floodplain at a lower streamflow than the original channel. Overall, the uncertainty of the sampling results indicates the complexity of sediment transport in a river and suggests a need for multisite, multifaceted, multiyear data, and tools to simulate those data to effectively evaluate river restorations.

Introduction

The Rice Creek Watershed District (RCWD) was interested in understanding the sediment transport dynamics of Rice Creek (fig. 1) which flows into Long Lake (fig. 1). Since Rice Creek and Long Lake have sediment-related water-quality impairments, RCWD has been tasked with improving these conditions. Rice Creek is listed on the U.S. Environmental Protection Agency 303(d) stream list for both fish and macroinvertebrates impairments (Minnesota Pollution Control Agency, 2021), and Long Lake is listed for phosphorus impairments. These impairments may be caused in part by past channelization of Rice Creek which increased sedimentation and degraded aquatic habitats. Channel modifications to Rice Creek, which began before 1937 (Emmons and Olivier Resources, Incorporated, 2008), and land-use disturbances associated with previous agricultural activities and urbanization resulted in an incised, unstable stream with high and erosive streambanks; this stream had abandoned much of its historical floodplain (fig. 2).

The RCWD began the Rice Creek Meander Restoration Project to improve channel and riparian area conditions and decrease sediment and nutrient delivery to Long Lake; the Rice Creek Meander Restoration Project was completed in 2005. The Middle Rice Creek Restoration Project (MRCRP) began in January of 2016 as a cooperative effort between the RCWD and the Minnesota Board of Water and Soil Resources (fig. 3). These restoration projects constructed meanders based on the channel sinuosity before anthropogenic disturbances to enhance the ability of Rice Creek to access the historical floodplain (fig. 2). The MRCRP added approximately 625 meters of channel length to Rice Creek (fig. 3). Although prealteration meanders could not be replicated exactly, aerial photographs of historical meanders and oxbow cutoffs were examined during the design process to match the historical channel and floodplain (fig. 3; Emmons and Olivier Resources, Incorporated, 2008; University of Minnesota, 2021).

Before the stream restoration, an on-channel sedimentation pond referred to as the Long Lake Inlet Facility (approximately 1,800 meters downstream from the

[1]U.S. Geological Survey.

[2]Rice Creek Watershed District.

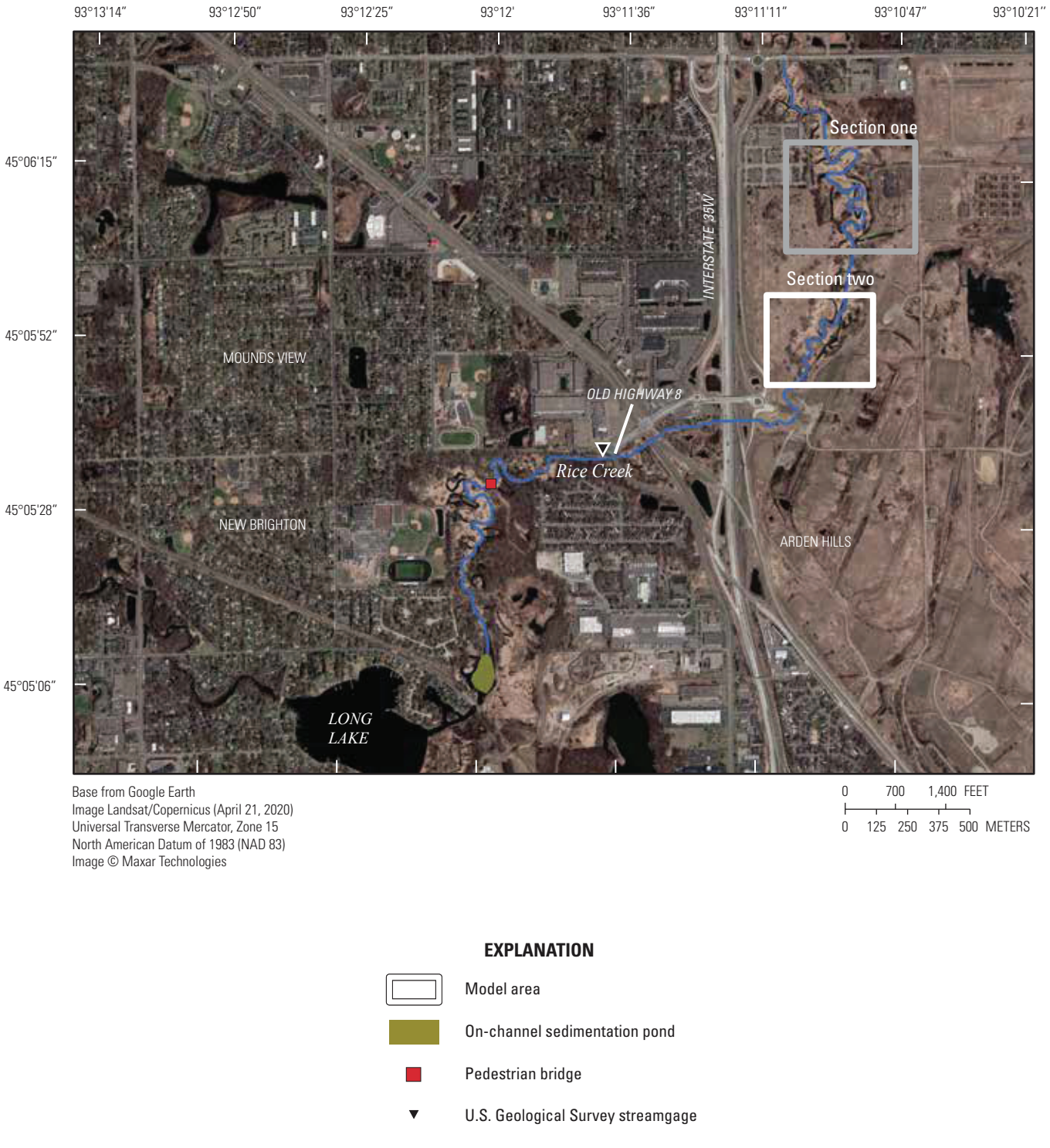

Figure 1. Study area that includes Rice Creek, sampling sites, stream restoration sections, on-channel sedimentation pond, and Long Lake.

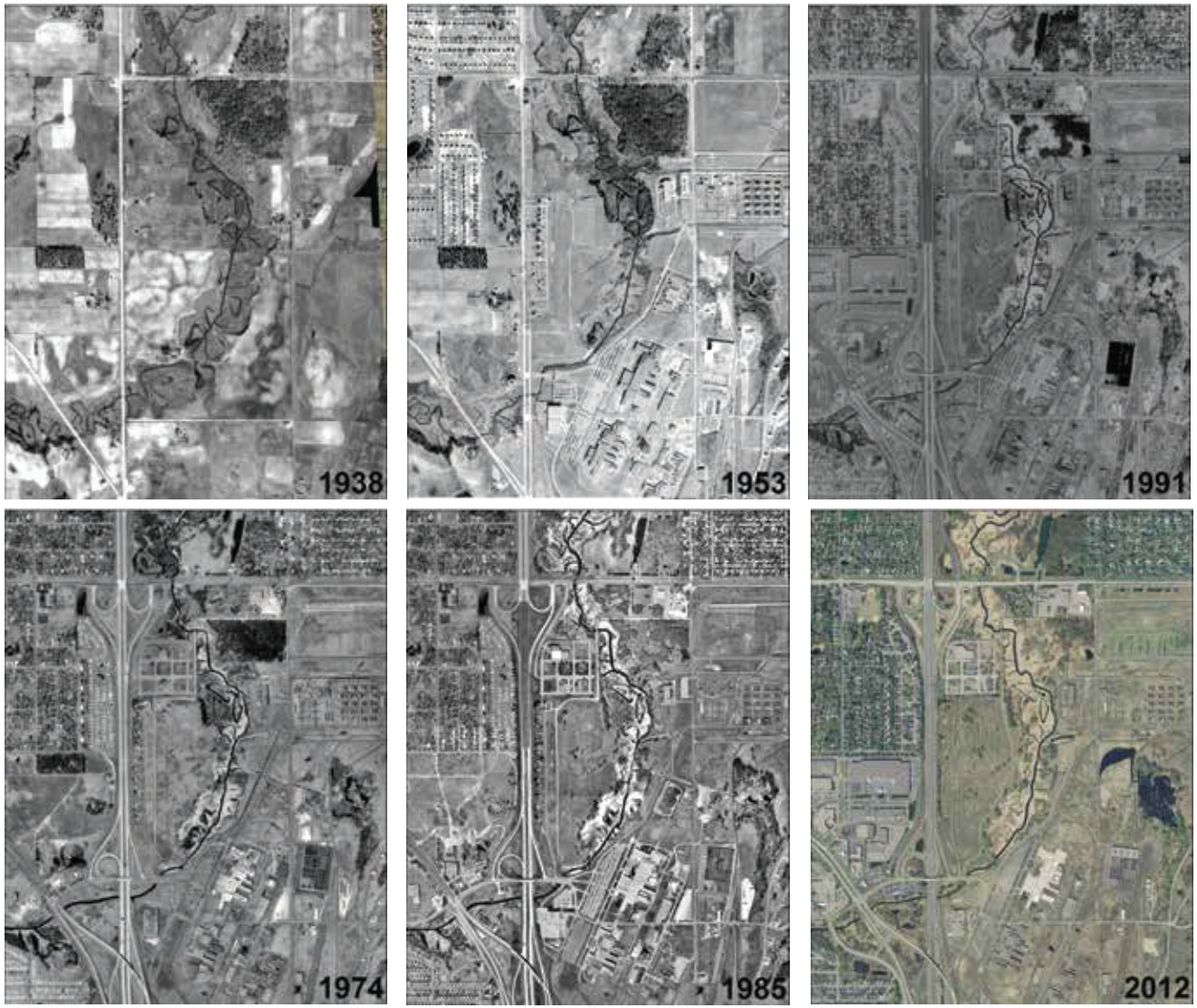

Aerial photographs are from the University of Minnesota 2021 webpage Minnesota Historical Aerial Photographs Online available at https://apps.lib.umn.edu/mhapo/

Figure 2. Historical aerial photographs of Rice Creek.

Figure 3. Map includes Middle Rice Creek Restoration Project and differentiates between restored and original Rice Creek channels and the surveyed and modeled area.

streamgage; fig. 1) was constructed in 1981 to reduce sediment deposition into Long Lake. The sediment intercepted by the Long Lake Inlet Facility needs to be periodically dredged, and this required maintenance is costly. The grain-size of sediment entering Long Lake from Rice Creek can affect the fill rates of the sedimentation pond and affect the downstream transport of phosphorus. Sand particles are larger and heavier and can be deposited more easily than finer grained sediments; however, the fine-grained sediments, which consist of silt, clay, and organic matter, tend to have higher total phosphorus concentrations, and these particles are more likely to stay in suspension and be transported downstream (Evans and others, 2004).

Increased phosphorus concentrations in lentic environments downstream from riverine inputs can contribute to seasonal hypoxia and formation of harmful algal blooms (Michalak and others, 2013; Sayers and others, 2016; Kreiling and others, 2019). In addition, reductions in phosphorus concentrations can lag behind efforts to reduce sediment because legacy sediments enriched with phosphorus may release stored phosphorus into the water column by diffusive flux from anoxic bottom sediment (Hamilton, 2012; Sharpley and others, 2013; Kreiling and others, 2019) or when sediments are physically disturbed by bottom-feeding fish, motorized boat activity, and wind mixing (Minnesota Pollution Control Agency, 2014). High phosphorus concentrations have been measured in Long Lake, and the south basin of Long Lake is currently impaired for aquatic recreation because of high nutrients; the north and south basins have phosphorus concentrations that exceed the State standard. The north basin typically has higher phosphorus concentrations than the south basin but is not assessed by State standards because of short residence times of water and because it is not classified as "lake" but as a "riverine basin" by State standards.

In alluvial streams, there is a functional relation among the hydraulic properties of flow and suspended sands and bedload; however, there is not a functional relation between suspended fines (wash load) and hydraulic properties of flow. Sand can either be transported as bedload or suspended by turbulent flow. The transport rate of suspended fines is usually a function of the supply made available. Suspended fines are normally delivered to the stream by overland flow, stormwater sewers, bank sloughing, and [or] bank erosion. In most streams, sediment transport and streamflow are not independent of one another, so it can be challenging to differentiate upstream changes in sediment supply from variability in streamflow year-to-year (Warrick, 2015).

The relation between streamflow and sediment transport can change during storm events. Hysteresis occurs when the relation between measured sediment (suspended and bedload) and streamflow changes between the rising and falling limbs of a streamflow hydrograph (Gray and Simões, 2008). In a bivariate plot comparing sediment and streamflow, hysteresis is indicated graphically by a loop in chronologically ordered data (Landers and Sturm, 2013). Clockwise hysteresis indicates higher sediment on the rising limb of the hydrograph than on the falling limb of the hydrograph. Conversely, counterclockwise hysteresis indicates higher sediment on the falling limb of the hydrograph compared to the rising limb of the hydrograph. The type of observed hysteresis can indicate antecedent conditions and mechanisms of sediment supply to the stream channel (Dean and others, 2020; Dean and others, 2016; Heidel, 1956; Kleinhans and others, 2007; Topping and others, 2000a; Topping and others, 2000b). In addition, alterations to distributions of boundary shear stresses within the channel caused by the scour and fill of the streambed can contribute to hysteresis (Rubin and others, 2020; Topping and others, 2021). Finally, hysteresis can also be caused by lags between flood hydrographs and the growth, decay, and downstream movement of sediment dunes along the bed of a river (Julien and others, 2002; Kleinhans and others, 2007; Shimizu and others, 2009; Topping and Wright, 2016). Hysteresis can make it difficult to develop relations between streamflow and measured sediment (suspended and bedload).

The U.S. Geological Survey (USGS), in cooperation with the RCWD, established a 10-year monitoring and flow modeling program. The monitoring and modeling program was intended to inform RCWD whether stream restoration efforts could improve water quality, reduce sediment loading, and minimize dredging costs. The monitoring included collecting suspended sediment concentrations (SSCs) and bedload samples in Rice Creek before and after stream restoration activities. Samples collected in 2010, 2011, and 2014 provided baseline data to evaluate the effects of future restoration activities. The MRCRP added stream meanders in Rice Creek above the study site location where the baseline data were collected. Post-stream restoration SSC and bedload samples were collected in 2018 and 2019 for comparison to pre-stream restoration data to evaluate changes in sediment transport. In addition, the pre-stream restoration channel, restored meander channels, and riparian areas surrounding the channels were surveyed using high-resolution survey equipment, and these data were used to develop flow models to evaluate the hydraulics and conveyance of the channel before and after the stream restoration.

Purpose and Scope

The purpose of this report is to assess changes in sediment loading, morphology of stream channels and riparian areas, and streamflow conditions after restoration activities that added constructed meanders to resemble historical channel conditions in Rice Creek upstream from Long Lake. Specifically, the report describes (1) the relations among SSC, sand, fines, bedload, and streamflow in Rice Creek for water years (WYs) 2010, 2011, 2014, 2018, and 2019, (2) annual total loads for WYs 2010 through 2019, and (3) model outputs from before and after stream restoration conditions.

Description of the Study Area

The Rice Creek Basin encompasses an area of approximately 482 square kilometers in the northeast Minneapolis-St. Paul Metropolitan area, Minnesota (Rice Creek Watershed District, 2017). The upper reaches of the Rice Creek Basin are largely undeveloped with extensive wetland complexes, and the lower reaches are fully urbanized (Arnston and others, 2004). Rice Creek flows through a chain of five shallow lakes starting at Peltier Lake and ending at Baldwin Lake and flows through several more wetland complexes. Middle Rice Creek flows from Baldwin Lake in Circle Pines to Long Lake in New Brighton, Minn (Emmons and Olivier Resources, Incorporated, 2008; fig. 1). These lakes and wetland complexes drive the hydrology of the study area because they provide water and sediment storage.

Rice Creek is located along the eastern edge of the Anoka Sand Plain, an area of surficial till and lacustrine sediments from several glacial advances and retreats during the most recent Quarternary glaciations (Cooper, 1935; Farnham, 1956; Wright, 1972a, b; Smith and others, 2017). The term Anoka Sand Plain is used to describe the sand-plain aquifer and associated valley-train deposits (Helgesen and Lindholm, 1977). Anoka Sand Plain sediments are highly complex because of the interaction of several distinct ice lobes over time and differential erosion that occurred between multiple advances and retreats of the Wisconsinan glaciation (Wright, 1972a, b; Smith and others, 2017); however, the predominant grain size of the upper outwash decreases from west to east (Helgesen and Lindholm, 1977). The Anoka Sand Plain generally is characterized by high evapotranspiration rates and sandy soils (Anderson, 1993). More specifically, the MRCRP is predominantly in soils that have a higher percentage of sands than silt (U.S. Department of Agriculture, 2021). Downstream from Interstate 35W, Rice Creek flows through Chaska silt loam soil which has a greater percentage of silt and fines than the upstream MRCPR location (U.S. Department of Agriculture, 2021).

Sampling Sites

The pre-stream restoration sediment monitoring site was colocated at a streamgage (U.S. Geological Survey station 05288580; fig. 1) below Old Highway 8 in Mounds View, Minn. (fig. 1). This location was not suited for sampling during elevated streamflows (greater than 300 cubic feet per second [ft^3/s]) because the water was too deep to safely collect a wading sample. A culvert located approximately 55 meters upstream (under Old Highway 8; fig. 1) of the streamgage was also not a suitable or safe option for deploying samplers that required a crane because of its configuration.

However, during the stream restoration (2016 through 2017), a pedestrian bridge (fig. 1) was installed approximately 665 meters downstream from the streamgage. There are no tributaries or confounding factors such as high streambanks between the streamgage and pedestrian bridge. At elevated streamflows, deploying a sampler with a crane from this pedestrian bridge was safe and effective during the post-stream restoration monitoring period. Ideally, the study would have been improved if there were two sampling sites directly upstream and downstream from where the stream restoration was planned to isolate the effects of the stream restoration and reduce uncertainty in the sample results. However, it was not possible to have two sampling sites at these locations because of funding constraints.

Survey Area

The survey area was approximately 1,100 meters upstream from the streamgage (fig. 1) in Arden Hills, Minn. The survey area included the furthest downstream restoration section and is labeled as “Section two” in figure 3. The surveyed area included the pre-stream restoration (light green color in the box in figure 3) and post-stream restoration (dark blue color in the box in figure 3) channels and extended beyond both channels into their respective floodplains. The pre-stream restoration streambanks and floodplain consisted mostly of reed canary grass while the post-stream restoration banks and floodplain consisted mostly of cattails.

Additional Observations

Rice Creek was modified downstream from the survey area by the Minnesota Department of Transportation to reroute it under Interstate 35W (fig. 3). The original channel is shown as a darker orange color in figure 3 and the rerouted channel is shown as a lighter orange color in figure 3. The rerouted channel was narrower than the original channel which increased flow velocities. During the study, streambank erosion was observed at the first meander streambank of this rerouted channel because of the increased flow velocities and shear stress. Later in the study, the meander streambank was reinforced with riprap to prevent erosion. While these modifications are downstream from the survey area, they did introduce some uncertainty when comparing conditions before and after the stream restoration; however, quantifying the effects of these modification on the study reach was not within scope of this investigation.

Methods of Data Collection and Analysis

Suspended sediment and bedload samples were collected at USGS streamgage station 05288580 during WYs 2010, 2011, and 2014 (pre-stream restoration) and downstream from the streamgage during WYs 2018 through 2019 (post-stream restoration). Samples were collected for a range of streamflows when the river was not covered by ice (open-water season). The collected samples were analyzed for SSCs and percentage of fines, which were used to calculate

suspended-sands concentrations (hereafter referred to as "sands"), and suspended-fines concentrations (hereafter referred to as "fines"), total bedload mass, and bedload particle-size distributions. The laboratory analyses are explained in the "Laboratory Analysis" section.

Sampling Methods

Water samples were collected using isokinetic samplers and depth-integrating techniques at equal-width increments (EWIs; Edwards and Glysson, 1999; Davis, 2005). For the collection of water samples, the stream width was divided into 10 EWIs. An isokinetic, depth-integrated sample was collected at the centroid of each increment following the procedures described in Edwards and Glysson (1999). Based on the river depth and velocity, samples from each centroid were collected with a DH-48 sampler lined with a 1-pint glass bottle during wadable streamflows or a D–74 sampler lined with either a 1-pint or 1-quart glass bottle during nonwadable streamflows (Davis, 2005). After the sampling event, the water samples collected from all the centroids of the stream transect were combined into one composite sample for laboratory analyses.

Bedload samples were collected concurrently with water samples. A BLH–84 pressure-differential bag sampler was used to collect bedload samples during wadeable streamflows, and a BL-84 was used during nonwadable streamflows (Davis, 2005). The mesh pore sizes of the bags used to collect the bedload samples varied from 0.112 to 0.5 millimeter (mm), depending on site conditions. The single EWI method was used to collect bedload samples (Edwards and Glysson, 1999). Samples were collected by starting near one streambank and collecting one sample at each of the 20 evenly spaced increments across the stream cross-section to the opposite bank. The bedload sampler rested on the streambed for 30 seconds at each increment. This process was repeated twice to obtain two separate samples. Bag samples were transferred into plastic containers and composited before laboratory analyses.

Surveying Methods

Ground surface elevation (GSE) data were collected at the downstream section of the Middle Rice Creek Restoration (fig. 1; Groten and others, 2022). Multiple survey techniques and equipment were used to collect elevation data. Elevations of the terrain above the water surface were collected using terrestrial laser scanning, airborne light detection and ranging (lidar; Minnesota Department of Natural Resources, 2012), real time kinematic (RTK) global navigation satellite system (GNSS) equipment, and a total station integrated with RTK-GNSS. Bathymetric data from the pre-stream and post-stream restoration channels were collected with an acoustic Doppler current profiler which measured the depths of the pre-stream and post-stream restoration channels. The depths were corrected to elevation using corresponding water surface elevations measured with RTK-GNSS equipment and processed with the Velocity Mapping Toolbox (Parsons and others, 2013; U.S. Geological Survey, 2021a).

Laboratory Analysis

Water samples were analyzed for SSC following method D3977–97 (Guy, 1969; American Society for Testing and Materials, 2000) and for the percentages of fines, by wet sieving, (Guy, 1969) at the USGS Sediment Laboratory in Iowa City, Iowa. Fines are defined as particles with a diameter less than 0.0625 mm and consists of silt and clay. Particles that have a diameter greater than or equal to 0.0625 mm and as much as 2.0 mm are classified as sands. The sands were calculated by taking the percentage of fines and multiplying it by the corresponding SSC value, dividing the product by 100, and subtracting the quotient from the SSC value. The fines were calculated by subtracting the calculated sands value from the corresponding SSC value.

Bedload samples were analyzed for total mass (grams) and particle-size distributions ranging from 0.0625 to 16 mm and included 9 sizes (Guy, 1969). Bedload samples were analyzed by USGS staff in Minnesota. Results from laboratory analyses are available in a USGS data release (Groten and others, 2022) and can be accessed from the USGS National Water Information System (NWIS) web page (U.S. Geological Survey, 2021c). Bedload transport (BL) was calculated using the following equation (Edwards and Glysson, 1999):

$$Qb = K \times (W/t) \times M \quad (1)$$

where

Qb is bedload transport, in tons per day;
K is a conversion factor of 0.381 for the types of samplers used for data collection (BL-84 and BLH-84 have a 3-inch-wide opening);
W is total sampling width of where the bedload samples were collected in the stream channel, in feet;
t is total time the sampler was on the bed, in seconds; and
M is total bedload mass of sample collected from all verticals sampled in the cross section, in grams.

Streamflow Data

Instantaneous (15-minute) and daily mean streamflow data are available at the USGS NWIS web page (U.S. Geological Survey, 2021c). The instantaneous streamflow values were used to develop simple linear regression (SLR) models. The daily mean streamflow values were used to

calculate bedload and suspended sediment loads. Daily mean streamflow values were also used as input to multidimensional flow models to calibrate and validate the models.

Data Analysis

Statistical analyses were completed and included the development of SLR models, testing the difference between regression slopes with the t-statistic, and testing the difference between the vertical offset parameter with analysis of covariance (ANCOVA). After development of the SLR models, select SLR models were used to compute daily and annual load estimates. Additional analyses included using the GSE points to develop multidimensional flow models to compare the hydraulics and conveyance of the pre-stream and post-stream restoration channels.

Development of Linear Regression Models

The suitability of streamflow and sediment relations was tested by doing ordinary least squares regression analyses (Helsel and others, 2020) using streamflow as an explanatory variable and SSC, fines, sands, BL, percent fines, and percent sands as the response variables. Different combinations of SLRs on untransformed and transformed data were tested. A level of significance (α) of 0.05 was used for all statistical analyses presented in this study.

The Surrogate Analysis and Index Developer Tool (Domanski and others, 2015) was used to develop SLR models and evaluate the accuracy of the models developed for estimating SSCs, fines, sands, BL, percent fines, and percent sands. Diagnostic plots, residual errors, and probability values (p-values) were examined to ensure the models met the assumptions of ordinary least squares regression analyses (Helsel and others, 2020; Groten and others, 2022). Streamflow, SSC, fines, sands, and BL were log transformed (base-10 logarithms), and bias-correction factors were applied (Duan, 1983) after the data were retransformed into the original units (Groten and others, 2022). The pre-stream and post-stream restoration SLR models' streamflow were normalized by the geometric mean of the streamflow values sampled to better characterize trends in the vertical offset (Warrick, 2015). The final selected SLR models were used to generate a time series of estimated SSC, fines, sands, and BL values and prediction intervals (Helsel and others, 2020; Groten and others, 2022). The following SLR model forms were used:

$$SSC,\ Fines,\ Sands,\ \text{or}\ BL\ =\ b_0(Q/Q_M)^{b_1} \times BCF \quad (2)$$

$$SSC,\ Fines,\ Sands,\ \text{or}\ BL\ =\ b_0(Q)^{b_1} \times BCF \quad (3)$$

$$\%Fines\ or\ \%Sands\ =\ b\,0\ \pm\ b\,1(Q) \quad (4)$$

where

SSC is the response variable suspended-sediment concentration, in milligrams per liter;
Fines is the response variable suspended-fines concentration, in milligrams per liter;
Sands is the response variable suspended-sand concentration, in milligrams per liter;
BL is the response variable bedload transport, in tons per day;
%Fines is the response variable percentage of fines in the corresponding SSC sample, in percent;
%Sands is the response variable percentage of sands in the corresponding SSC sample, in percent;
b_0 is the vertical offset parameter;
b_1 is the slope of the explanatory variable;
Q is the explanatory variable streamflow, in cubic feet per second;
Q_M is the geometric mean of the streamflow data sampled (Warrick, 2015), in cubic feet per second; and
BCF is the bias-correction factor (Duan, 1983).

The pre-stream and post-stream restoration SLR slopes and vertical offset parameters in equation 2 were tested for significance with the t-statistic and ANCOVA, respectively. Select SLR models were then used to estimate daily loads as described in the next section.

Daily and Annual Load Estimates

Daily mean estimates of SSC, BL, and corresponding 90 percent prediction intervals (Domanski and others, 2015) were calculated from the final SLR models (Groten and others, 2022). Fines and sands were calculated by taking the corresponding daily mean streamflow that was used to estimate SSC and applying it to equation 4 to estimate the percentage of fines. This percent was divided by 100, the quotient was multiplied by the corresponding SSC estimate to calculate the fines, and the calculated fines was subtracted by the corresponding SSC estimate to calculate the sands. Daily suspended-sediment loads (SSL) were estimated using the following equation (Porterfield, 1972):

$$SSL = Q \times SS \times c_f \quad (5)$$

where

SSL is the estimated daily mean suspended-sediment load, in tons per day;
Q is the daily mean streamflow, in cubic feet per second;
SS is the estimated daily mean suspended-sediment concentration, suspended-fines concentration, or suspended-sands concentrations, in milligrams per liter, from the final simple linear regression models; and

c_f is a coefficient (0.0027) that converts the units of streamflow and SSC, fines, or sands into tons per day and assumes a specific gravity of 2.65 for sediment.

The SSL and BL were summed to report the total daily load, and all the estimated daily loads were summed to calculate total annual loads for each year of the study (WYs 2010 through 2019).

Development of Multidimensional Flow Models

The International River Interface Cooperative (iRIC) surface-water modeling software and the FaSTMECH solver (iRIC, 2021; Nelson and McDonald, 1996; Nelson, 2016) were used to develop, calibrate, validate, and run pre-stream and post-stream restoration two-dimensional flow models. The iRIC software and FaSTMECH solver are available through the International River Interface Cooperative web page (iRIC, 2021). The purpose of this modeling effort was to provide spatially distributed quantities throughout the modeled domain to quantitatively evaluate the pre-stream and post-stream restoration channels for important metrics such as (1) water-surface elevations (WSEs), (2) water depths, (3) water velocity, and (4) shear stress. These metrics were used to evaluate what streamflows have access to the floodplains and changes in pre-stream and post-stream restoration channel morphologies, and to make sediment-transport inferences between the pre-stream and post-stream restoration channels.

The GSE data were used as input to the iRIC software. Erroneous GSE points were identified by comparing to the surrounding points and removed. Interpolated GSE points were manually added in the iRIC software to better define the channel. The grids were developed by digitizing the centerline by following the channel curvature and specifying the width of the channel and the number of grid cells in the streamwise and cross-stream direction. The pre-stream and post-stream restoration grids had cell sizes of 1 meter by 1 meter. Since the sinuosity of the post-stream restoration channel was greater than the pre-stream restoration channel, the width of the post-stream restoration grid was constrained mostly to the channel. The post-stream restoration grid did not extend very far into the floodplain because when a grid with a wider cross-stream distance was tested in the iRIC software, the grid overlapped in the channel bends because of the high sinuosity of the channel in these areas. A template was used to map the elevations of the GSE points to the developed grids and is similar to a nearest-neighbor search with a specified length and width that follow the curvature of the developed grid.

The streamgage height (GH) and the downstream measured WSEs of the pre-stream and post-stream restoration channels were used to calculate an offset (Groten and others, 2022). The offset was used to correct the GHs in the streamgage's rating tables so they could be used as rating curves in the pre-stream and post-stream restoration models. The GH used in the models' rating curves (Groten and others, 2022) were corrected to be the WSE at the downstream location of the modeled domain. Since there are no tributary inflows and there is a short distance between the modeled domain and the streamgage, the streamflow at the streamgage was used for both rating curves in the models (Groten and others, 2022).

Grid elevations and streamflow were input into the pre-stream and post-stream restoration models. The models were calibrated for a given streamflow and measured WSEs. Sensitivity analyses tested the model parameters: roughness and lateral eddy viscosity (LEV) with the lowest root-mean-square error (RMSE) between measured and modeled WSEs. The parameter values with the lowest RMSE were used to calibrate the models. The post-stream restoration model was independently validated to a different streamflow, but the pre-stream restoration was not because the channel was decommissioned during the study. Finally, seven pre-stream restoration and seven post-stream restoration models were run.

Streamflow, Suspended Sediment, and Bedload Results

The amount of rainfall has a direct effect on streamflow. The measured rainfall was above the historical mean (27.6 in. for base period 1939 through 2000; National Oceanic and Atmospheric Administration, 2021) at St. Paul, Minn. for each WY in the study (WYs 2010 through 2019). During the study, WY 2019 had the greatest measured rainfall, and the lowest measured rainfall was in WY 2013 (National Oceanic and Atmospheric Administration, 2021). Because the rainfall was greater in WY 2019, the highest annual mean streamflow (137 ft^3/s) was observed in WY 2019 (U.S. Geological Survey, 2021c). Further comparing streamflow and rainfall, WY 2010 was unique because it had the lowest annual mean streamflow (U.S. Geological Survey, 2021c) but had 6 more inches of rain than the lowest measured rainfall in WY 2013.

An important consideration when comparing the data collected during the pre-stream and post-stream restoration monitoring was the varying ability to obtain samples at elevated streamflows during these periods. This difference made it difficult and introduced some uncertainty when comparing the pre-stream and post-stream restoration datasets. Samples could be collected at elevated streamflows during the post-stream restoration monitoring period because a pedestrian bridge was installed downstream from the streamgage (fig. 1). There were 4 samples collected above 290 ft^3/s during the post-stream restoration sampling period while only 1 sample was collected above 290 ft^3/s during the pre-stream restoration monitoring period (fig. 4). Overall, the streamflows that coincided with sampling events were higher during the post-stream restoration than the pre-stream restoration monitoring period (fig. 5); however, the pre-stream restoration monitoring period observed some higher streamflow events (highest daily mean streamflow of 395 ft^3/s in WY 2014; fig.4).

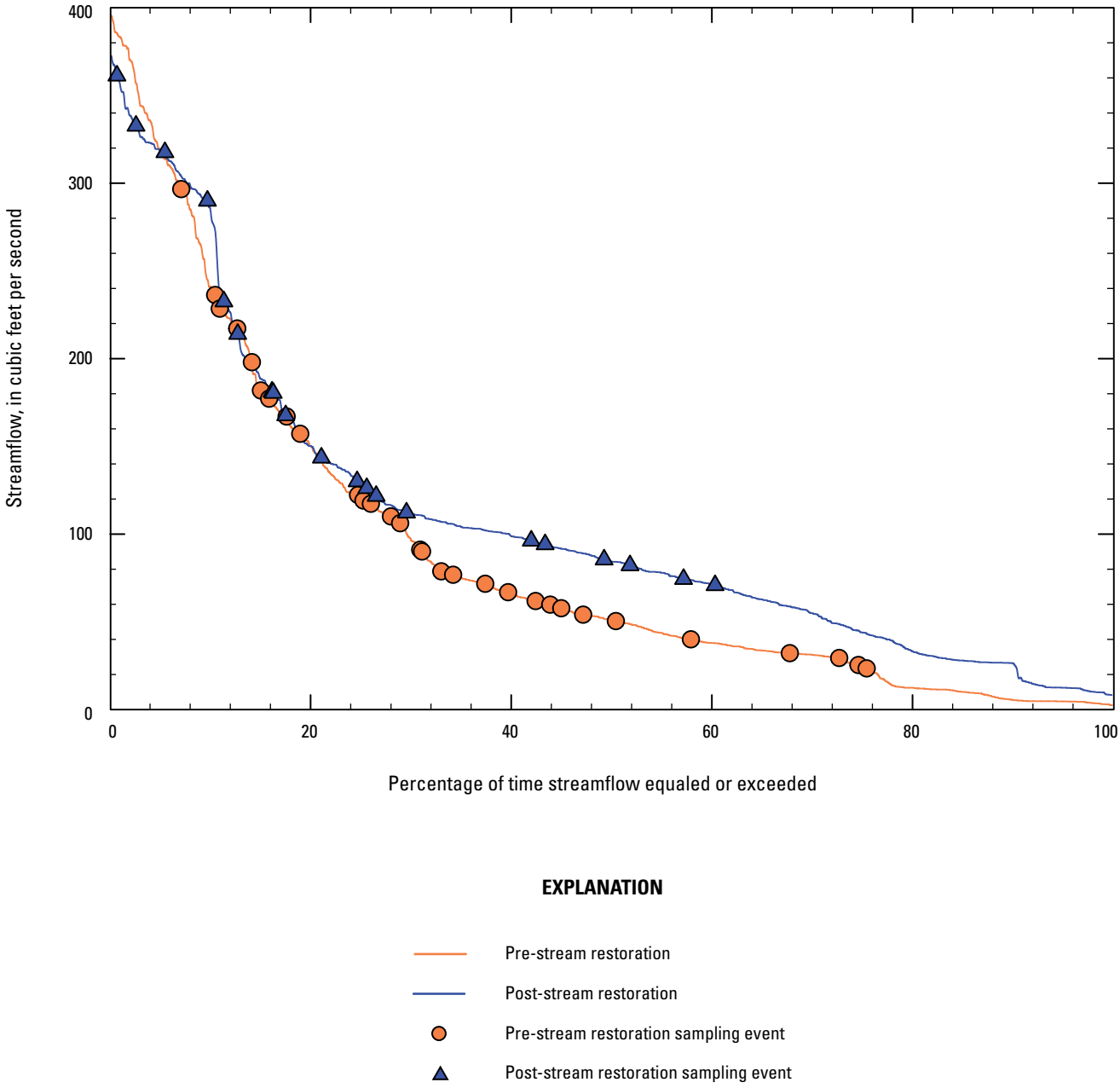

Figure 4. Flow-duration curves and associated sampling events at Rice Creek, water years 2010 through 2019. Pre-stream restoration (water years 2010, 2011, and 2014) and post-stream restoration (water years 2018 through 2019).

Another important consideration was the low streamflows (less than 53.7 ft^3/s) sampled during the pre-stream restoration monitoring period. There were 8 samples collected below 53.7 ft^3/s during the pre-stream restoration monitoring period while no samples were collected below 70.8 ft^3/s during the post-stream restoration monitoring period. A final and important consideration, the streamgage's GH-streamflow relation (rating curve) used to estimate streamflow has had multiple shifts and new rating curves developed because of the degradation of the stream channel (Erich Kessler, U.S. Geological Survey, oral commun., 2021). This phenomenon also made it difficult and introduced uncertainty when comparing the pre-stream and post-stream restoration datasets because the channel is a potential source of sediment at pre-stream and post-stream restoration sampling locations.

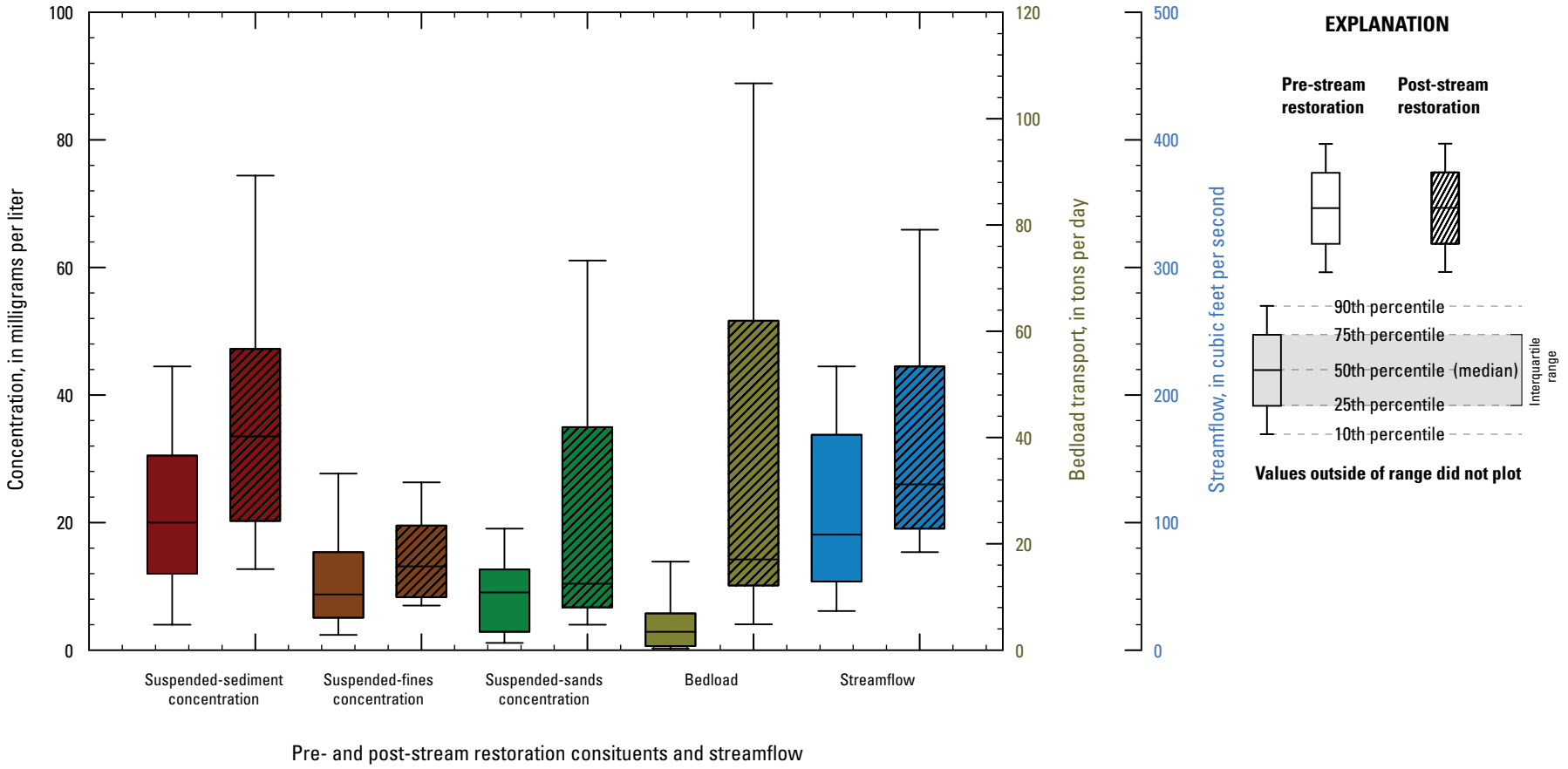

Figure 5. Measured suspended-sediment concentration, suspended-fines concentration, suspended-sands concentration, bedload, and streamflow at Rice Creek, pre-stream restoration (water years 2010, 2011, and 2014) and post-stream restoration (water years 2018 through 2019).

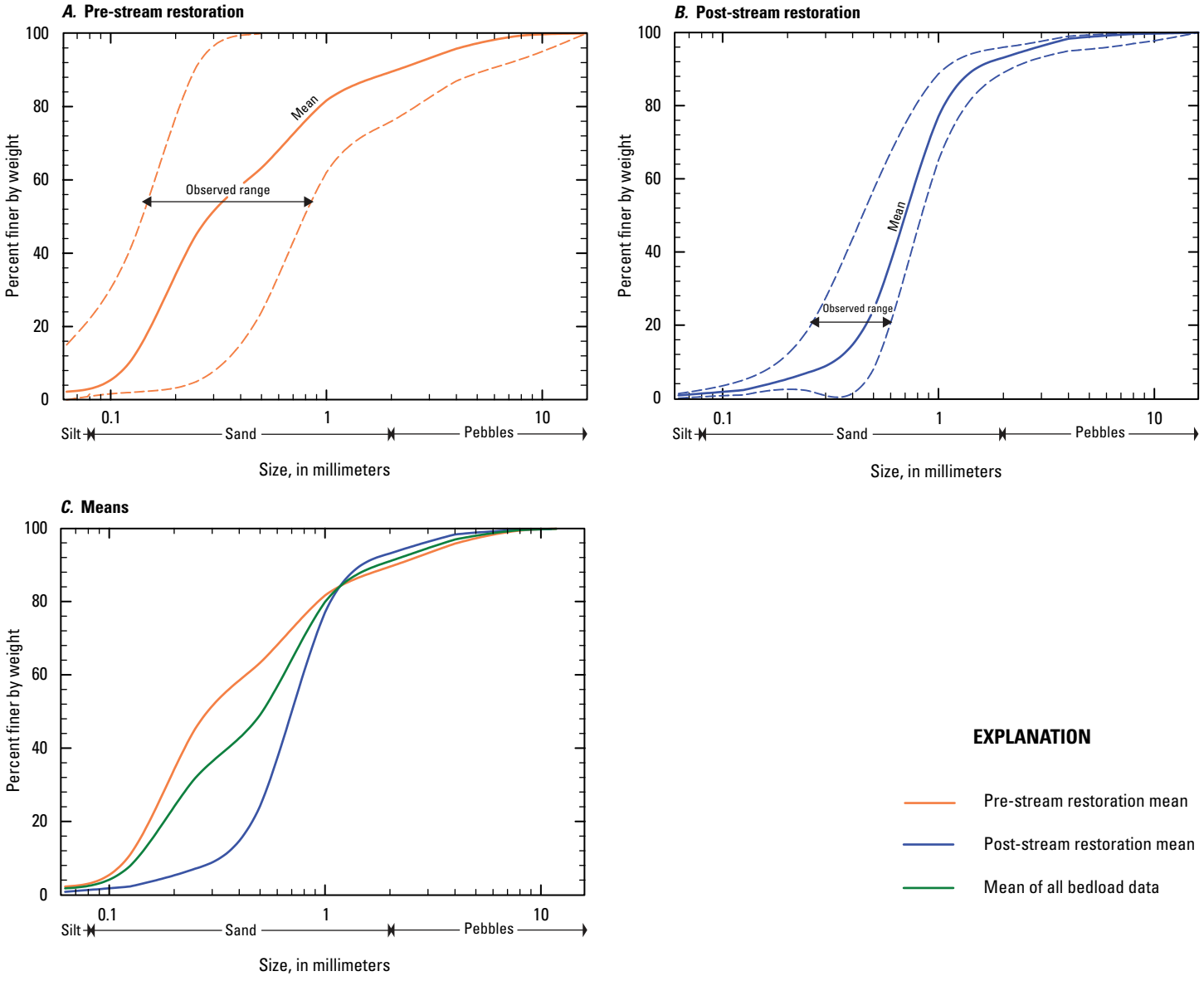

Figure 6. Cumulative-frequency distribution of mean and range of particle sizes in bedload samples at Rice Creek, *A*, pre-stream restoration (water years 2010, 2011, and 2014), *B*, post-stream restoration (water years 2018 through 2019), and, *C*, mean of bedload data.

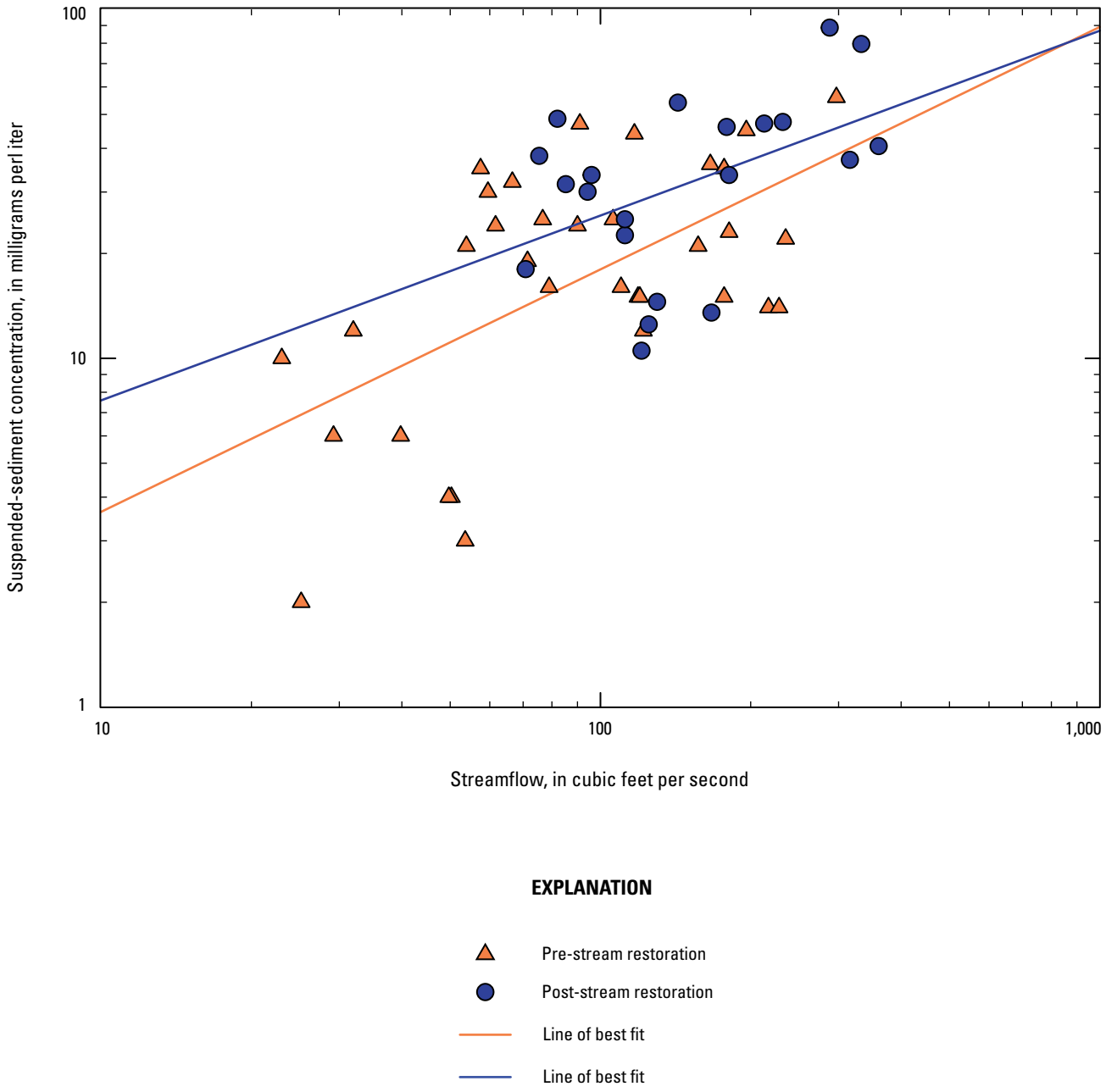

Figure 7. Relations among suspended-sediment concentration and streamflow at Rice Creek, pre-stream restoration (water years 2010, 2011, and 2014) and post-stream restoration (water years 2018 through 2019).

For all constituents monitored (SSC, fines, sands, BL) and streamflow, the post-stream restoration median values were higher than the pre-stream restoration values (fig. 5). The higher measured post-stream restoration values were a result of elevated streamflows and the ability to sample these streamflows during this monitoring period. The difference between the median pre-stream and post-stream restoration fines was less than all the other constituents measured (fig. 5). The percentage of suspended fines and suspended sands was approximately 50 percent for both periods. When comparing Rice Creek to other sites across Minnesota, Rice Creek had a higher percentage of suspended sand than 13 other sites in a statewide sediment study (Ellison and others, 2014).

Most bedload particles were larger for the post-stream restoration monitoring period (fig. 6). This was a result of elevated streamflows, higher energy to transport the larger sized particles, and the ability to sample elevated streamflows during the post-stream restoration monitoring period; however,

Table 1. Summary of linear regression models for pre-stream and post-stream restoration sediment sampling at Rice Creek, water years 2010, 2011, and 2014 (pre-stream restoration), 2018 through 2019 (post-stream restoration), and 2010 through 2019 (combined).

[n, number of samples; $Q_{GM,}$ geometric mean of streamflow data sampled; R^2, coefficient of determination; SLR, simple linear regression; p-value, probability value; t-stat, t-statistic tests the difference between SLR slopes[b]; ANCOVA, analysis of covariance; SSC, suspended-sediment concentration in milligrams per liter; pre-stream restoration, dataset collected during water years 2010, 2011, and 2014 and used for analyses; %, percent; Q, streamflow in cubic feet per second; <, less than; --, not computed; post-stream restoration, dataset collected during water years 2018 through 2019 and used for analyses; combined, dataset collected during water years 2010, 2011, 2014, 2018, and 2019 and used for analyses; fines, suspended-fines concentration; sand, suspended-sand concentration; BL, bedload transport]

Dataset	n	Q_{GM}	SLR model	Standard error	R^2	Average model standard percentage error	SLR p-value	t-stat	t-stat p-value	ANCOVA[e] p-value
Streamflow—SSC model										
Pre-stream restoration	34	89	$SSC = 16.6\left(\frac{Q}{Q_{GM}}\right)^{0.695^b} \times 1.21^c$	0.293	0.34W	75.8	<0.01	-0.570	0.571	<0.001
Post-stream restoration	21	147	$SSC = 31.6\left(\frac{Q}{Q_{GM}}\right)^{0.53^b} \times 1.12^c$	0.232	0.211	57.4	<0.05			
Combined	55	--	$SSC = 0.67^d(Q)^{0.739^b} \times 1.19^c$	0.274	0.383	70.0	<0.01	--	--	
Streamflow —Fines model										
Pre-stream restoration	26	117	$Fines = 11.2\left(\frac{Q}{Q_{GM}}\right)^{-0.575^b} \times 1.21^c$	0.268	0.184	68.0	<0.05	-0.039	0.969	0.304
Post-stream restoration	21	147	$Fines = 13.2\left(\frac{Q}{Q_{GM}}\right)^{-0.587^b} \times 1.07^c$	0.174	0.369	41.7	<0.01			
Combined	55	--	$Fines = 4.3^d(Q)^{0.183^b} \times 1.29^c$	0.329	0.026	88.0	0.242	--	--	
Streamflow—Sand model										
Pre-stream restoration	34	89	$Sand = 6.4\left(\frac{Q}{Q_{GM}}\right)^{1.12^b} \times 1.23^c$	0.289	0.58	75.7	<0.01	0.947	0.348	<0.001
Post-stream restoration	21	147	$Sand = 14.1\left(\frac{Q}{Q_{GM}}\right)^{1.44^b} \times 1.19^c$	0.285	0.568	73.3	<0.01			
Combined	55	--	$Sand = 0.02^d(Q)^{1.25^b} \times 1.22^c$	0.287	0.62	74.0	<0.01	--	--	
Streamflow—BL model										
Pre-stream restoration	22	115	$BL = 2.3\left(\frac{Q}{Q_{GM}}\right)^{1.52^b} \times 1.71^c$	0.480	0.408	155.0	<0.01	0.039	0.969	<0.005
Post-stream restoration	12	202	$BL = 22.9\left(\frac{Q}{Q_{GM}}\right)^{1.54^b} \times 1.18^c$	0.289	0.636	74.6	<0.01			
Combined	34	--	$BL = 0.0003^d(Q)^{2.01^b} \times 1.68^c$	0.495	0.558	163.0	<0.01	--	--	
Streamflow—Percent Fines and Sands model										
Percent Fines	55	--	$\%Fines = 79.8 - 0.205(Q)$	14.5	0.58	--	<0.01			
Percent Sands	55	--	$\%Sands = 20.2 + 0.205(Q)$	14.5	0.58	--	<0.01			

[a]Vertical offset parameter equivalent to the middle of the SSC, Fines, Sands, or BL sample distribution.

[b]Slope parameter of SLR line used for t-stat.

[c]Bias correction factor or "smearing" estimator is used to correct retransformation bias of regression estimates (Duan, 1983).

[d]Vertical offset parameter of SLR line.

[e]ANCOVA test to see if there is a significant difference in the vertical offset parameters[a] of the dependent variable for the equal slopes regression models comparing to the adjusted means of the factor groups.

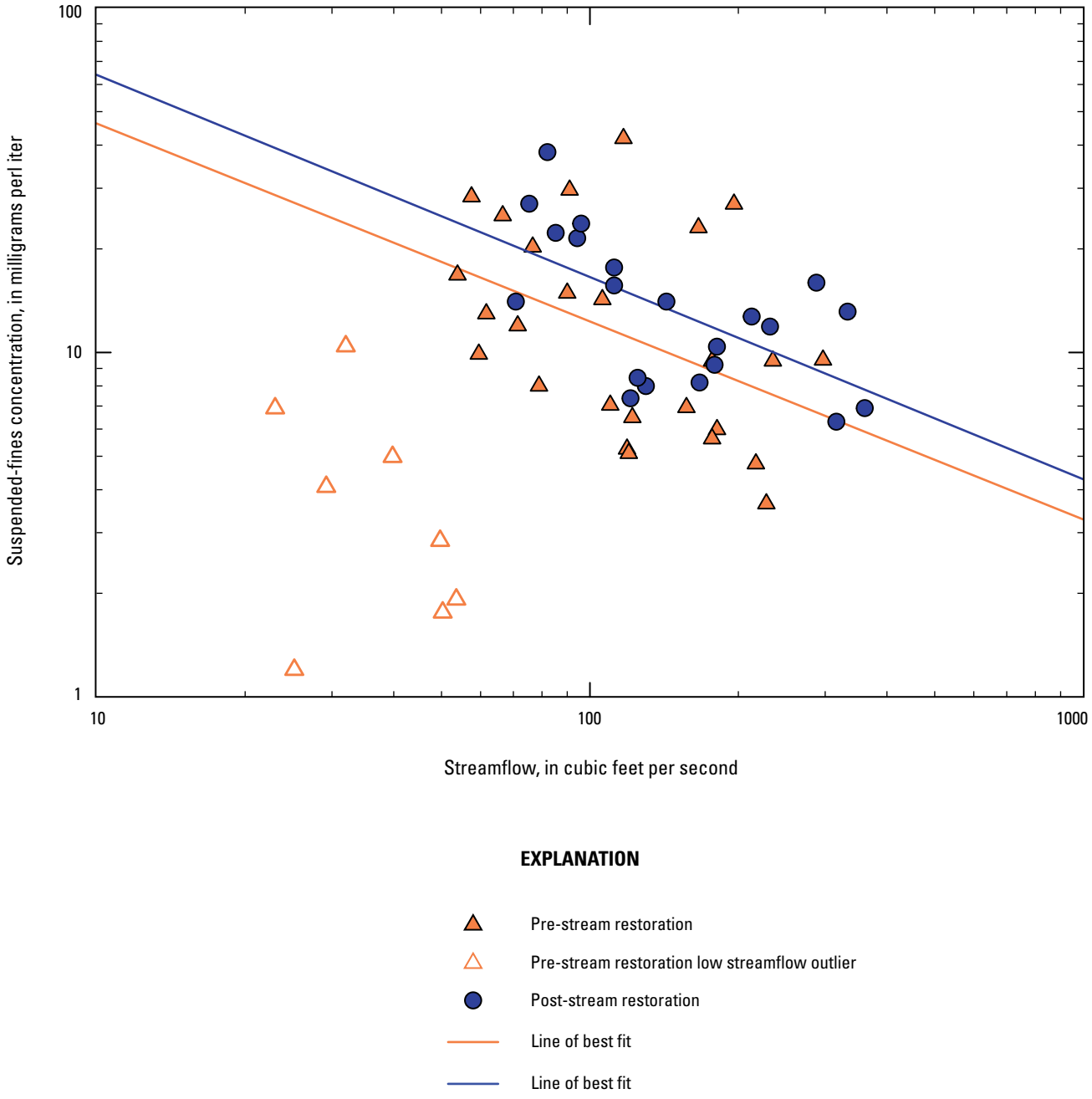

Figure 8. Relations among suspended-fines concentration and streamflow at Rice Creek, pre-stream restoration (water years 2010, 2011, and 2014) and post-stream restoration (water years 2018 through 2019).

for grain sizes above 1 mm the pre-stream restoration bedload was slightly larger, but the observed range of approximately [~] 4 percent was small above 1 mm between the pre-stream and post-stream restoration datasets (fig. 6*C*). Alternatively, the observed particle size range was larger for sizes less than 1 mm, and the post-stream restoration bedload was larger than the pre-stream restoration bedload for sizes below 1 mm for most measured particle sizes (fig. 6). Overall, the BL particle sizes measured in this study were small considering that a small percentage (~10 percent) were particles larger than sand (greater than 2 mm; fig. 6).

Simple Linear Regression Models

Fourteen SLR models were developed to estimate six variables: SSC, fines, sands, BL, percent fines, and percent sands (table 1). Three models were developed for SSC, fines,

sands, and BL from the pre-stream restoration (WYs 2010, 2011, and 2014), post-stream restoration (WYs 2018 and 2019), and the combined (WYs 2010, 2011, 2014, 2018, and 2019) datasets (table 1).

Suspended-Sediment Concentration Models

Three statistically significant SLR models were developed from the pre-stream restoration, post-stream restoration, and combined datasets (table 1) to estimate SSCs. A t-test calculated the t-statistic and determined that there was not a statistically significant difference between the pre-stream and post-stream restoration SLR slopes (table 1). ANCOVA determined there was a statistically significant difference in the vertical offset parameters of the dependent variable (table 1) since there is a significant difference in the adjusted means of the pre-stream and post-stream restoration. The post-stream restoration vertical offset (31.6 mg/L; table 1) was greater than the pre-stream restoration vertical offset (16.6 mg/L; table 1). The pre-stream restoration slope was greater and in the same directions as the post-stream restoration slope, but the difference was not statistically significant.

Two streamflows were compared to illustrate the variability in the data. At approximately 300 ft^3/s, there was a wider range of measured values (from ~40 to ~90 mg/L) observed than at 100 ft^3/s (fig. 7); however, the logarithmic scale of the graph makes it appear as though there was a wider range at 100 ft^3/s, but the actual measured range was smaller (from ~10 to ~40 mg/L at ~100 ft^3/s). The wide range of SSCs at approximately 300 ft^3/s was likely because of hysteresis, which was likely caused by the dynamic evolution of dunes in transport. The combined SLR model (table 1) was used to estimate daily mean SSCs and SSLs for WYs 2010 through 2019 because the combined model represented the whole range of flows and included fines and sands.

Suspended-Fines Concentration Models

Two statistically significant SLR models that estimated fines were developed from the pre-stream and post-stream restoration datasets (table 1). Eight values (fig. 8) below 53.7 ft^3/s were removed from the dataset because they were biasing the pre-stream restoration SLR model, so it was not comparable with the post-stream restoration SLR. A t-test determined that there was not a statistically significant difference between the pre-stream and post-stream restoration SLR slopes (table 1). ANCOVA determined there was not a statistically significant difference in the vertical offset parameters of the dependent variable (table 1) since there was no significant difference in the adjusted means of the pre-stream and post-stream restoration. Both pre-stream and post-stream restoration slopes were negative and were similar values. The post-stream restoration vertical offset parameter was slightly greater than that of the pre-stream restoration vertical offset parameter (table 1). The combined dataset, including the eight pre-stream restoration samples below 53.7 ft^3/s, was used to develop a combined SLR, but a statistically significant model could not be developed.

The negative pre-stream and post-stream restoration SLR slopes suggest that fines supply is being depleted with increasing streamflow (table 1; fig. 8). The reduction in suspended fines with increasing streamflow may also mean reduced phosphorus with increasing streamflows since phosphorus can bind to fine grained sediments (Stone and Murdoch, 1989), but this cannot be concluded definitively because phosphorus was not measured as part of this study. The post-stream restoration fines SLR model had the lowest error (0.174) amongst all the12 SLR models developed (table 1).

Suspended-Sand Concentration Models

Three statistically significant SLR models were developed from the pre-stream restoration, post-stream restoration, and combined datasets (table 1) to estimate sands. A t-test determined there was not a statistically significant difference between pre-stream and post-stream restoration SLR slopes (table 1). ANCOVA determined there was a statistically significant difference in the vertical offset parameters of the dependent variable (table 1) since there was a significant difference in the adjusted means of the pre-stream and post-stream restoration. The post-stream stream restoration vertical offset (14.1 mg/L; table 1) was greater than the pre-stream restoration vertical offset (6.4 mg/L; table 1) while the slopes of the pre-stream and post-stream restoration SLR models were similar (table 1; fig. 9).

Even though the SLR models developed were significant, the variance of all three models was high (table 1; fig. 9). The variance was likely because of hysteresis caused by the dynamic evolution of dunes in transport. Dunes would have the most effect on the sands amongst the three suspend-sediment constituents (SSC, fines, sands).

Bedload Models

Three statistically significant SLR models were developed from the pre-stream, post-stream restoration, and combined datasets (table 1) to estimate BL. A t-test determined that there was not a significant difference between the regression slopes of the pre-stream and post-stream restoration SLR models (table 1). ANCOVA determined there was a significant difference in the vertical offset parameters of the dependent variable (table 1) since there was a significant difference in the adjusted means of the pre-stream and post-stream restoration. The post-stream stream restoration vertical offset (22.9 tons per day; table 1) was greater than the pre-stream restoration vertical offset (2.3 tons per day; table 1) while the slopes of the pre-stream and post-stream restoration SLR models were very similar (table 1; fig. 10).

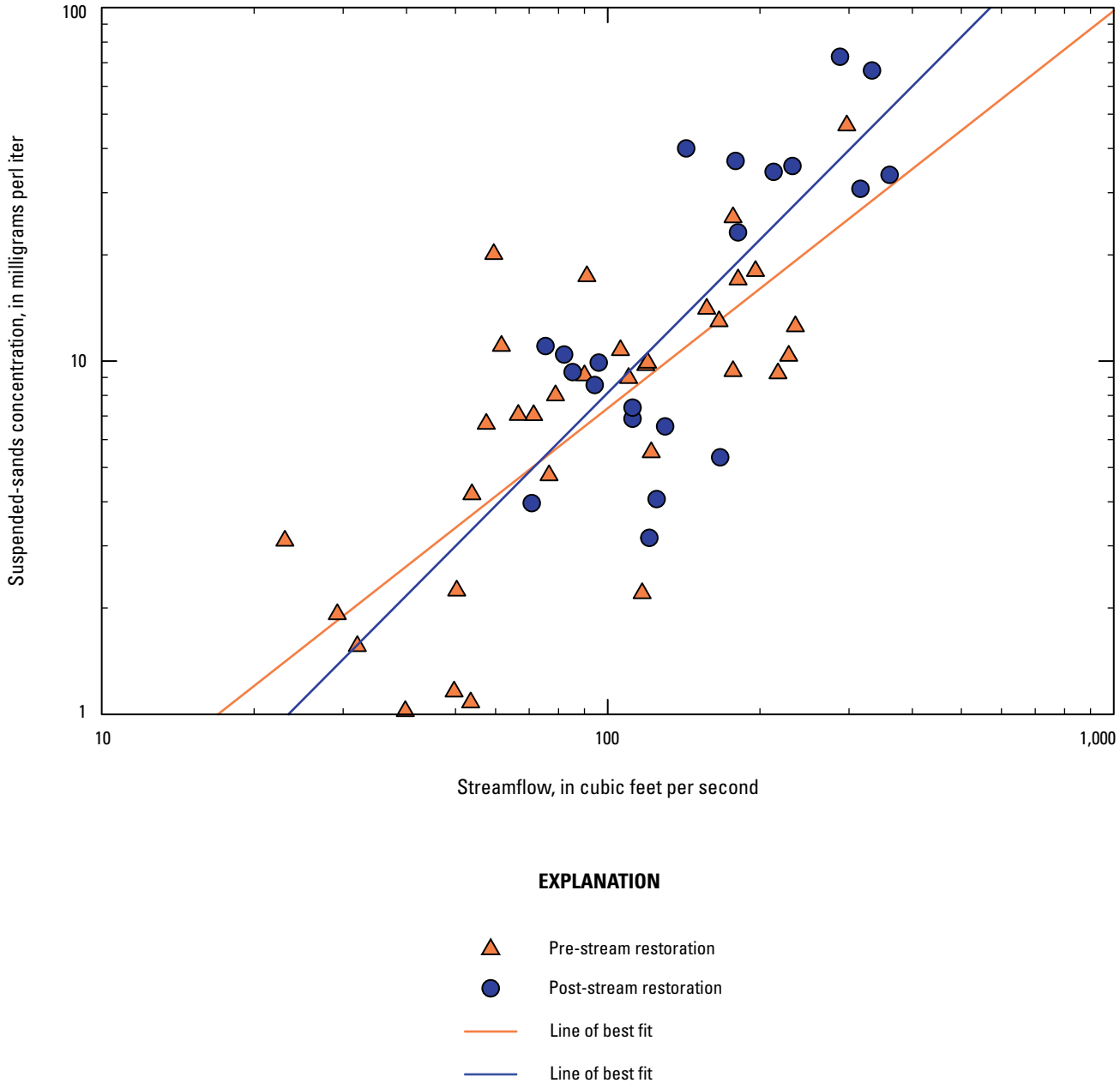

Figure 9. Relations among suspended-sands concentration and streamflow at Rice Creek, pre-stream restoration (water years 2010, 2011, and 2014) and post-stream restoration (water years 2018 through 2019).

The post-stream restoration SLR model error was less than the pre-stream restoration and combined SLR models (table 1**)**. This was likely caused by there being fewer bedload samples in the post-stream restoration dataset, so less variability was measured. Variability can be observed in the pre-stream restoration dataset which had more bedload samples (fig. 10**)**. Measuring bedload with the samplers and sampling methods used during this study can be challenging and highly variable because of the hydraulic efficiency of the samplers (Childers, 1999), inadvertently scooping the streambed, and loss of the bedload sample out of the nozzle after returning to water surface because of back pressure. In addition, the variability of bedload measurements can be exacerbated when dunes are present because BL varies along the dune with the trough having the lowest BL and the crest having the highest BL (Edwards and Glysson, 1999). To better represent the variability, the combined SLR model was used to estimate BL as part of the total load computations for WYs 2010 through 2019.

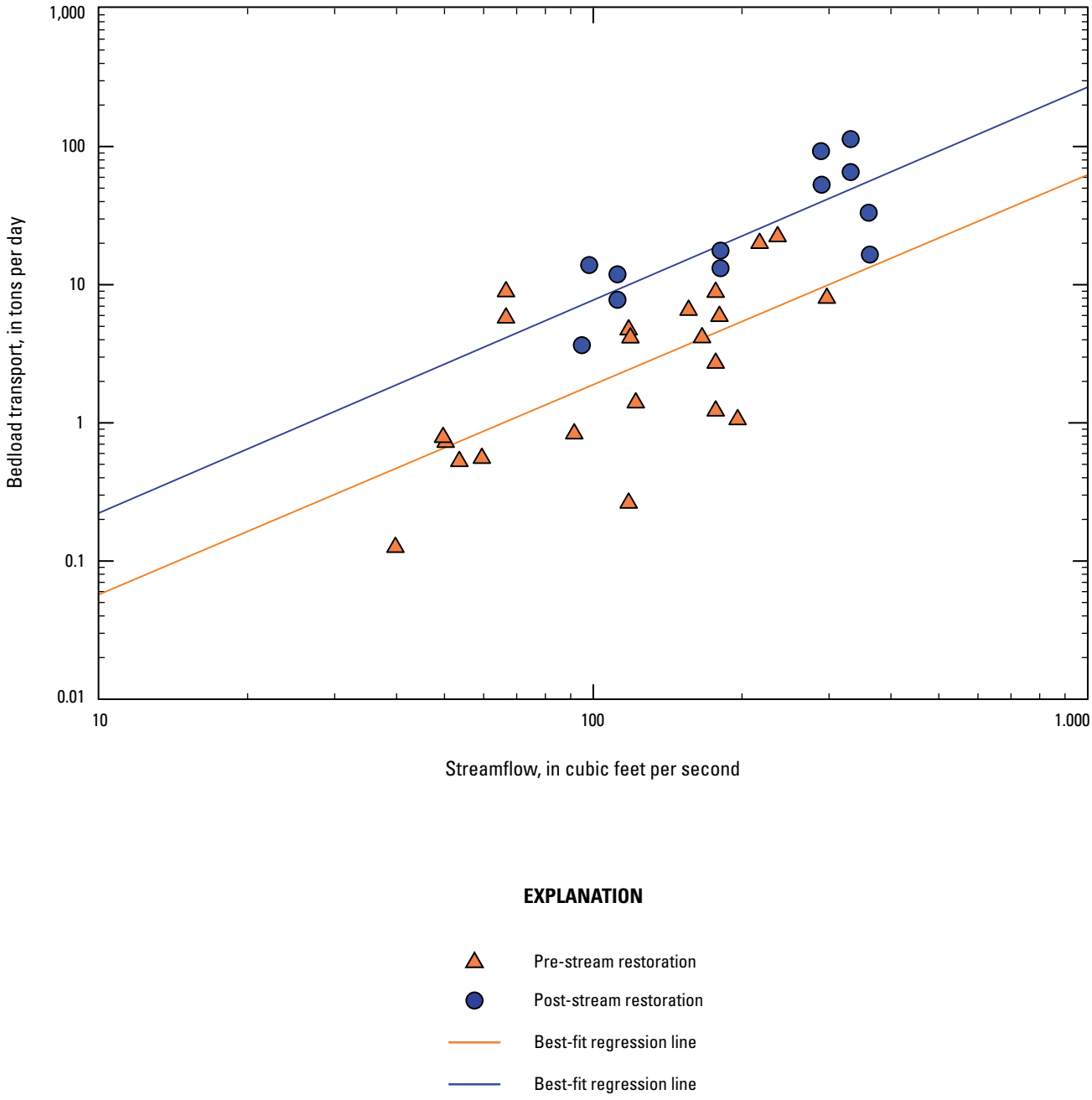

Figure 10. Relations among bedload transport and streamflow at Rice Creek pre-stream restoration (water years 2010, 2011, and 2014) and post-stream restoration (water years 2018 through 2019).

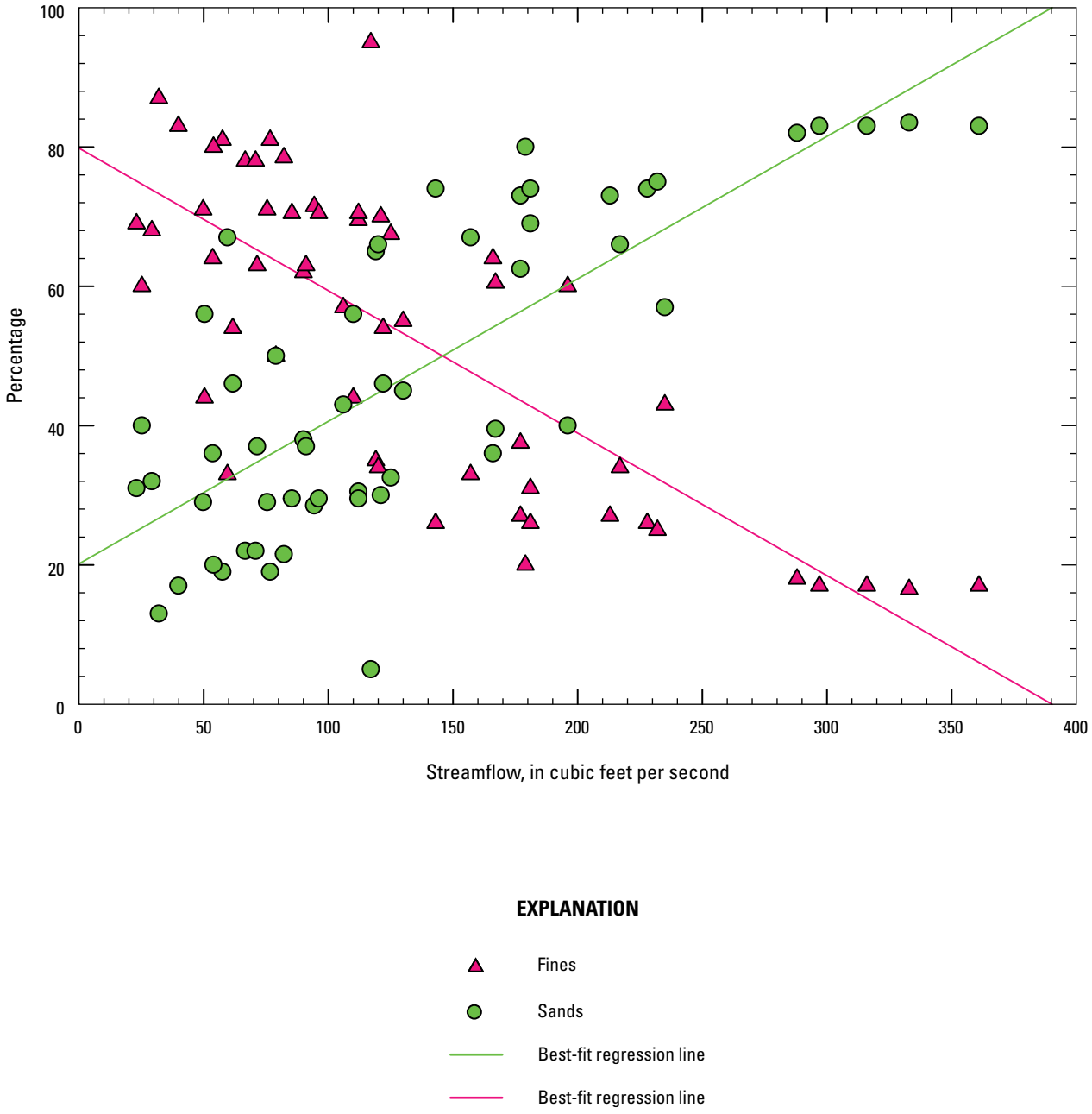

Figure 11. Relations among percent fines and sands and streamflow at Rice Creek, water years 2010, 2011, 2014, 2018, and 2019.

Table 2. Estimated suspended fines load, suspended sands load, bedload, and total loads at Rice Creek, water years 2010 through 2019.

[all loads are in tons per day]

Water year	Suspended fines load	Suspended sands load	Total suspended sediment load[a]	Bedload	Total load[b]
2010	480	300	780	510	1,290
2011	1,400	2,200	3,600	3,000	6,600
2012	630	640	1,270	950	2,220
2013	900	1,200	2,100	1,700	3,800
2014	860	4,450	5,360	4,900	10,260
2015	810	800	1,610	1,200	2,810
2016	1,500	1,500	3,000	2,200	5,200
2017	1,700	2,200	3,900	3,200	7,100
2018	1,000	880	1,880	1,400	3,280
2019	1,500	4,100	5,600	4,900	10,500

[a]Calculated by adding the suspended fines and sands together.

[b]Calculated by adding the total suspended sediment load to the bedload.

Percent Fines and Sands Models

Two significant SLR models were developed to estimate the percent fines and fines (table 1; fig. 11). Two SLR models were developed even though having both is redundant. The SLR models are redundant because they are the inverse of one another and are documented for illustration purposes. The percent fines SLR model has a negative slope while the percent sands SLR model has a positive slope. Since they are the inverse, only one was used to calculate fines and sands from the corresponding SSC which was explained in "Daily and Annual Load Estimates" section.

Estimation of Loads

The lowest total annual load and total annual streamflow was WY 2010 while WY 2019 had the highest total annual load and total annual streamflow (fig. 12). During the 10-year monitoring period (WYs 2010 through 2019), the mean BL contribution to the total load was approximately 40 percent while the mean SSL contribution to the total load was approximately 60 percent. The BL and suspended sand contribution to the total load increased with greater total annual streamflows because of more streamflow results in more energy for bedload and suspended sand transport (fig. 12). Bedload and sand are heavier than fines, so there will be a systematic increase in total loads when streamflows increase because there is more shear stress to transport the heavier particles. Higher streamflows also possibly depleted the supply of suspended fines, and there was a greater supply of suspended sands than suspended fines in all years except WYs 2010 and 2018 (table 2; fig. 11). WYs 2014 and 2019 had the biggest difference between suspended sands and fines with sands being greater (table 2; fig. 12) because peak streamflows were highest (445 and 375 ft^3/s, respectively) for these two WYs during the 10-year monitoring period.

Since middle Rice Creek flows out of a chain of lakes and wetland complexes, sediment transport at the upstream end of middle Rice Creek is low to negligible because of the low gradient. Because of the geologic material Rice Creek flows through, there was a consistent supply of fine sands; therefore, there was not a reduction but an increase in SSC, sand, and bedload during the post-stream restoration monitoring period because of higher streamflows. The RCWD assumed that middle Rice Creek's supply of sediment came from the original channel's high streambanks and the channel bottom. Suspended fines are driven more by the upstream supply than the energy of water. Another potential driver for the negative relations between streamflow and fines was a dilution effect: the supply of suspended fines to Rice Creek are from overland run-off or from stormwater sewers and the supply would cease when rainfall events ended; however, the supply of fines could have been greater if the stream had not been restored because of elevated streamflow and shear stress on the higher streambanks. Suspended sand and bedload increased during the post-stream restoration monitoring period. Because the transport of suspended sands and bedload are more dependent on the energy of moving water than the suspended fines, the greater streamflows during the post-stream restoration monitoring period and the consistent supply of sand are likely reasons why the sand and bedload increased; however, there are many interrelated factors that control sediment transport, and observed differences in pre-stream and post-stream restoration sediment transport could be from changes in streamflow, sediment supply, or both.

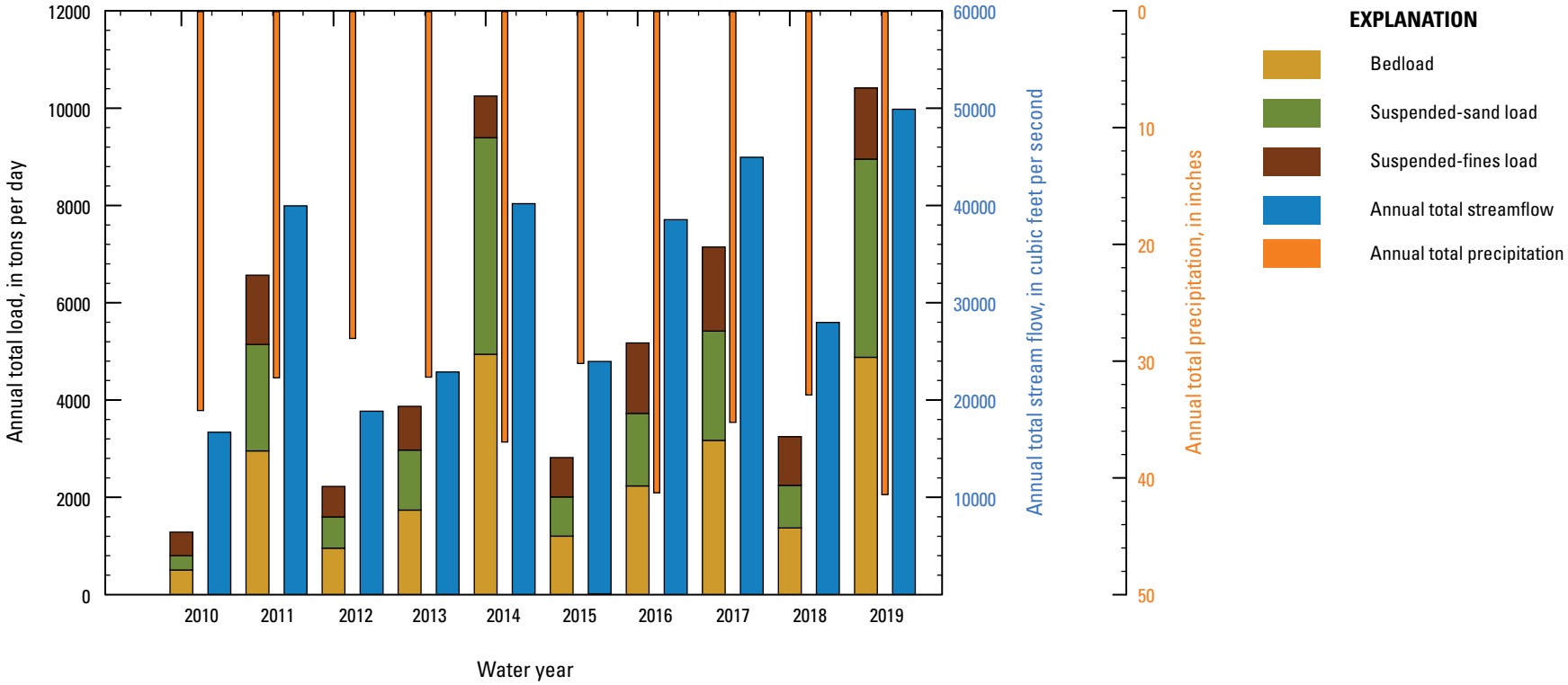

Figure 12. Estimated total annual loads, suspended sediment and bedload, measured streamflow, and measured rainfall at Rice Creek, water years 2010 through 2019.

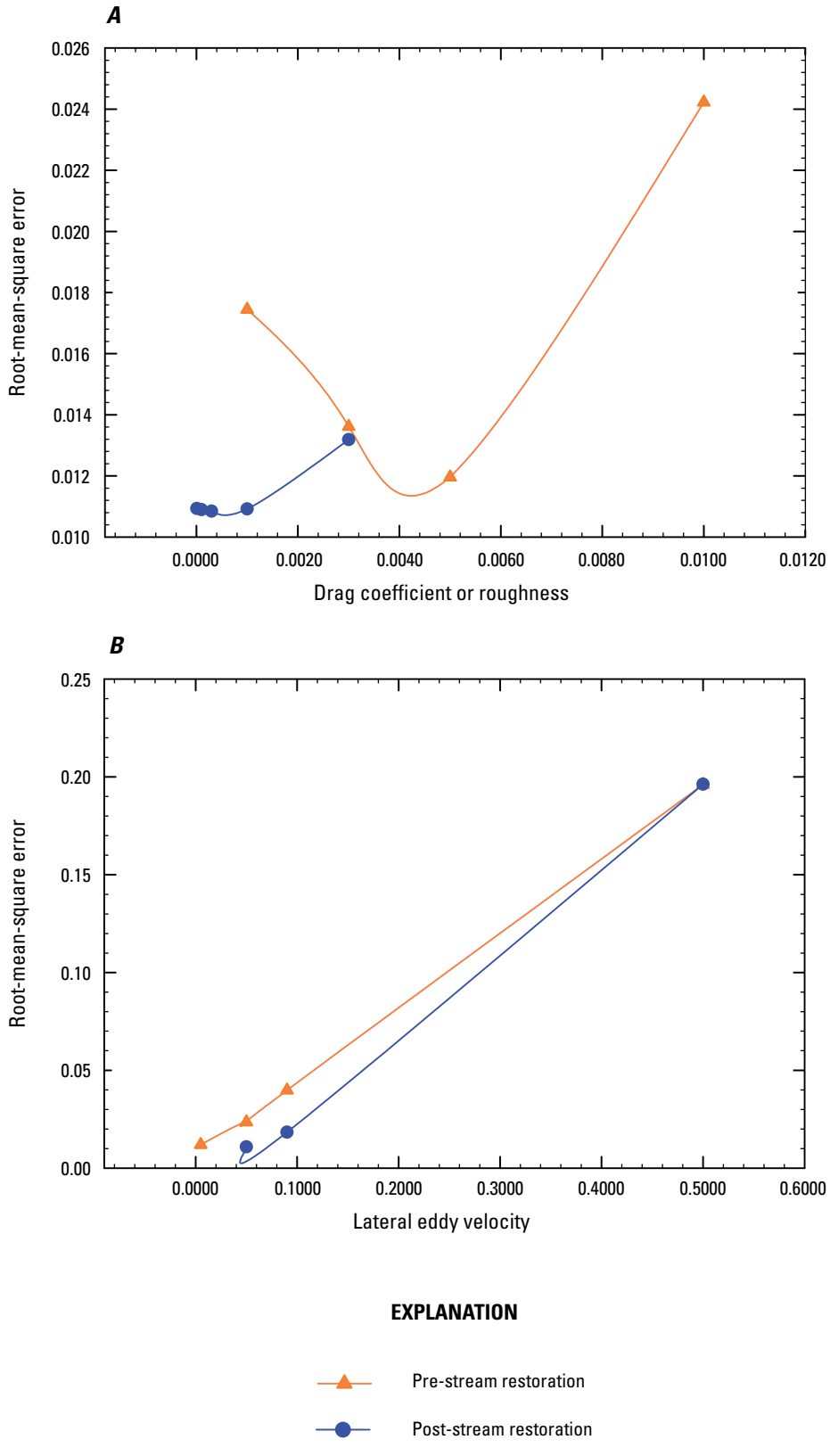

Figure 13. Sensitivity analysis of pre-stream and post-stream restoration model parameters, *A,* drag coefficient or roughness and, *B*, lateral eddy velocity versus root-mean-square-error (measured versus modeled water surface elevations).

Table 3. Select calculation conditions and final model parameters for pre-stream and post-stream restoration models.

[LEV, lateral eddy viscosity; WSE, water surface elevation; 1D, one dimensional]

Model	Discharge type	Stage type	Roughness type	Roughness distribution	Roughness	Constant LEV	Initial WSE	Iterations
Pre-stream restoration	Constant	Rating curve	Drag coefficient	Constant	0.005	0.005	1D Step-backwater	1,000
Post-stream restoration	Constant	Rating curve	Drag coefficient	Constant	0.0003	0.05	1D Step-backwater	1,000

Multidimensional Flow Models

Two FaSTMECH models were developed, calibrated, and run for multiple streamflow scenarios for pre-stream and post-stream restoration channel morphologies. Groten and others (2021) includes all GSEs, measured WSEs, grids, rating curves, calibration, validation, model run, and model result files.

Calibration and Validation

The pre-stream restoration model was developed and calibrated to a streamflow of 56 ft^3/s and WSEs measured on December 5, 2017. The results of a sensitivity analysis are shown in figure 13. Roughness and lateral eddy viscosity (LEV) parameters were adjusted to achieve the lowest RMSE between measured and modeled WSEs (fig. 13). The final selected parameters are documented in table 3. The pre-stream restoration rating table from December 5, 2017, with corrected GH was used as the rating curve in the pre-stream restoration model (Groten and others, 2022).

The post-stream restoration model was developed and calibrated to a streamflow of 310 ft^3/s and WSEs measured on May 3, 2019. The sensitivity analysis results are shown in figure 13. Roughness and LEV parameters were adjusted to achieve the lowest RMSE between measured and modeled WSEs (fig. 13). The final selected parameters are documented in table 3. The post-stream restoration corrected rating table from March 17, 2021, with corrected GH was used in the post-stream restoration model (Groten and others, 2022). The model was validated at a flow of 145 ft^3/s November 18, 2019 (Groten and others, 2022), with a RMSE of 0.0623 between measured and modeled WSEs (Groten and others, 2022).

Figure 14 illustrates the extent of flooding along the post-stream restoration floodplain compared to the modeled domain at the calibration streamflow of 310 ft^3/s on May 3, 2019. The hydrologic technician attempted to measure WSEs in the stream channel but was not able to access the channel in certain areas because of standing water in the floodplain. Where the hydrologic technician could not access the channel, the technician went to areas in the floodplain with stable footing to measure the WSE. The extent of the modeled grid is shown in black and blue on figure 14. Wet points in the modeled grid are shown in blue, and dry points are shown in black. Blue circles with a black outline indicate the locations where the WSE was measured. Note the distances between the grid and measured WSEs; at one point the measured WSE was approximately 60 meters from the grid on figure 14. Since it was confirmed that flooding extended past the modeled domain, the entire floodplain could not be modeled because the width of the grid predominantly included the channel. The measured WSEs illustrate the spatial extent of water in the floodplain. The post-stream restoration model can predict which streamflows access the floodplain but not the spatial extent of the flooding.

Model Runs

Seven streamflows were input into the pre-stream and post-stream restoration models to generate 14 model output files (Groten and others, 2022). The model runs were for streamflows of 50, 100, 150, 200, 250, 300, and 400 ft^3/s. The WSE and water depths at the seven streamflows were compared to visually determine bankfull streamflows for the two periods. Bankfull streamflows were visually determined from model output to be approximately 250 ft^3/s for the pre-stream restoration channel and approximately 150 ft^3/s for the post-stream restoration channel (figs. 15*C* and *B*, respectively). In figure 15*A*, it seems like water is in the pre-stream restoration floodplain, but these are distinct features (vegetated point bars and standing waters from an inlet) near the channel, and one is because of a boundary condition at the top of the modeled domain. A streamflow of 150 ft^3/s was confirmed to be near bankfull for the restored channel because the validation data that was collected on November 18, 2019, at 145 ft^3/s indicated that water was on the floodplain; however, this could have been standing water from previous streamflows that exceed bankfull streamflow. In addition, the cattails along the streambanks and in the floodplain might provide easier access to the floodplain because of their stem density. These factors make it difficult to determine a single bankfull streamflow. Bankfull streamflow is likely variable along the reach. Overall, the model results indicate a reduction of bankfull streamflow (approximately 100 ft^3/s) between the pre-stream and post-stream restoration channels, which was a goal of the restoration design to have connection to the floodplain by lowering the streambanks.

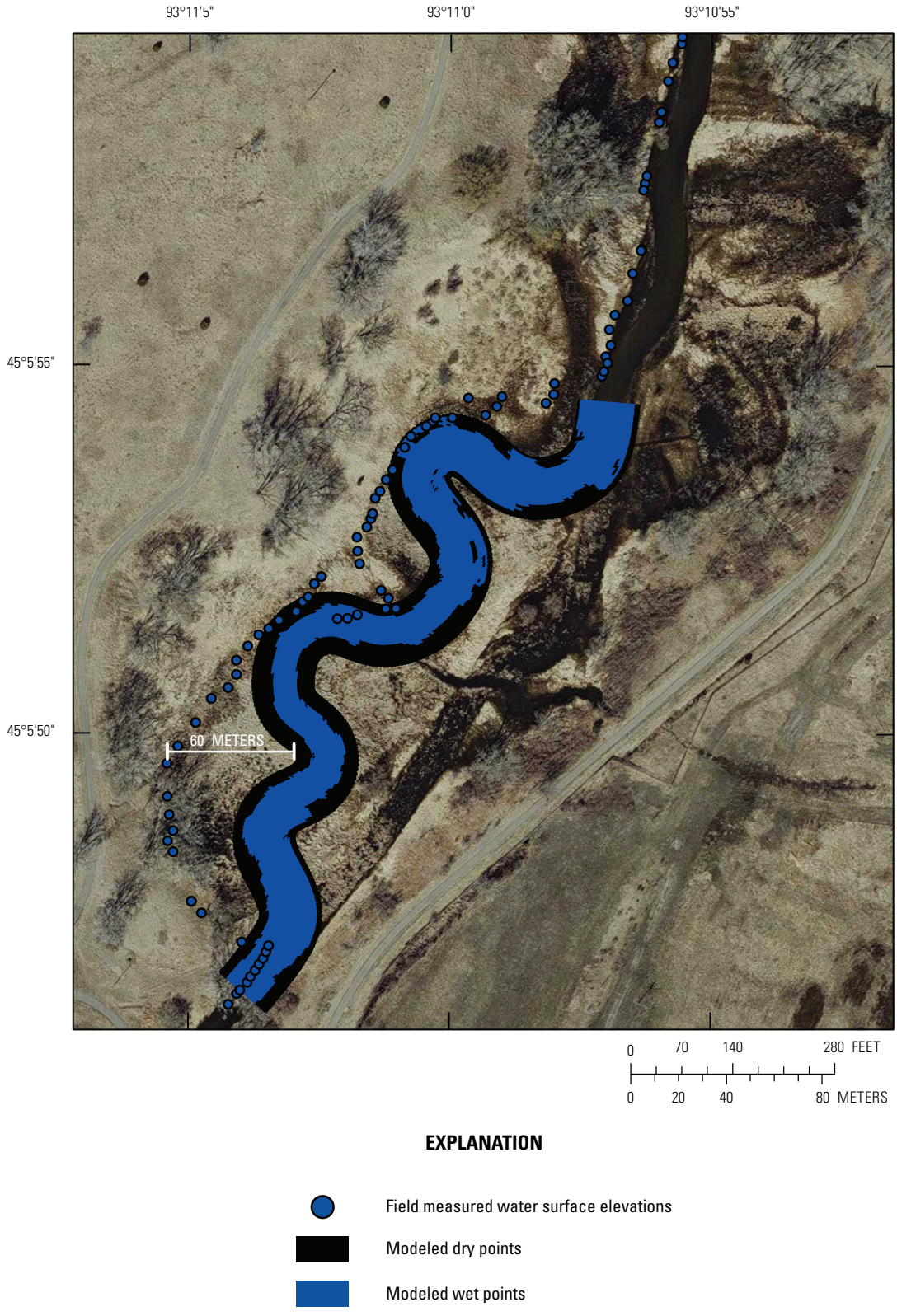

Figure 14. Extent of flooding on May 3, 2019, to illustrate the distance between modeled grid and measured water surface elevations in certain areas of the post-stream restoration area.

Figure 15. Modeled water depths pre-stream (*A*, *C*, *E*) and post-stream (*B*, *D*, *F*) restoration at three streamflows (150, 250, and 400 cubic feet per second, respectively).

B. Modeled water depths post-stream restoration

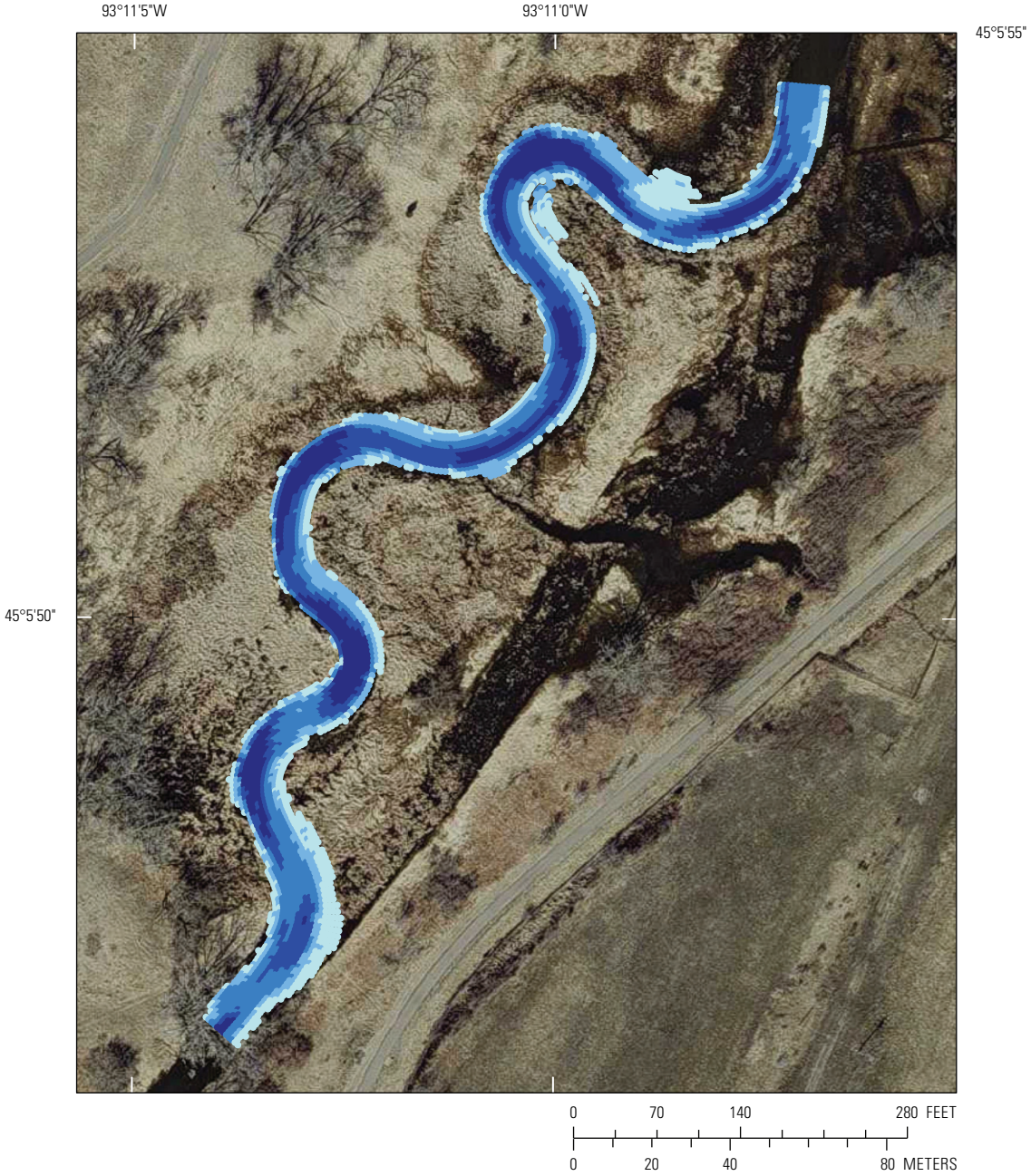

Figure 15.—Continued

C. Modeled water depths pre-stream restoration

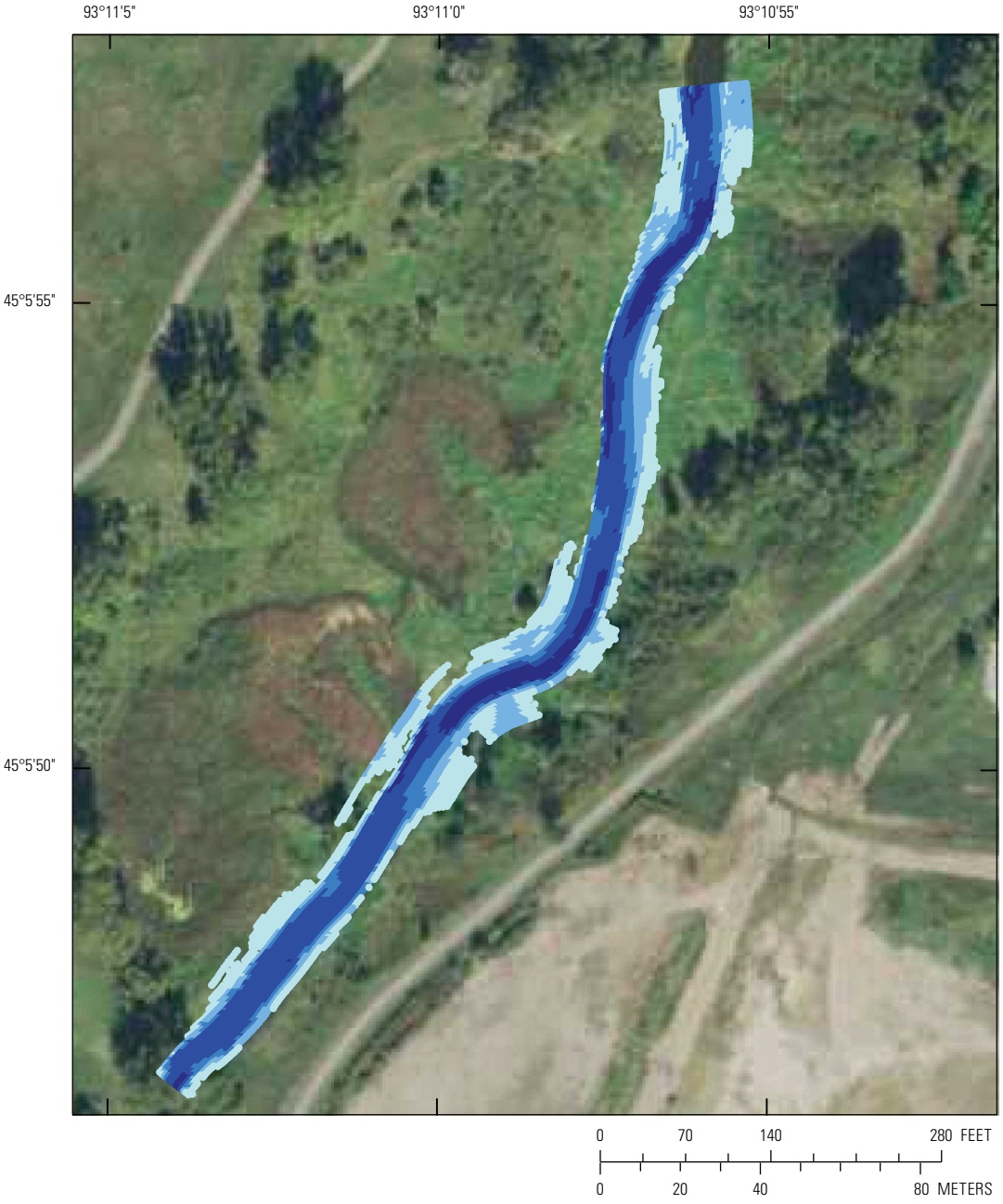

Figure 15.—Continued

D. Modeled water depths post-stream restoration

Figure 15.—Continued

E. Modeled water depths pre-stream restoration

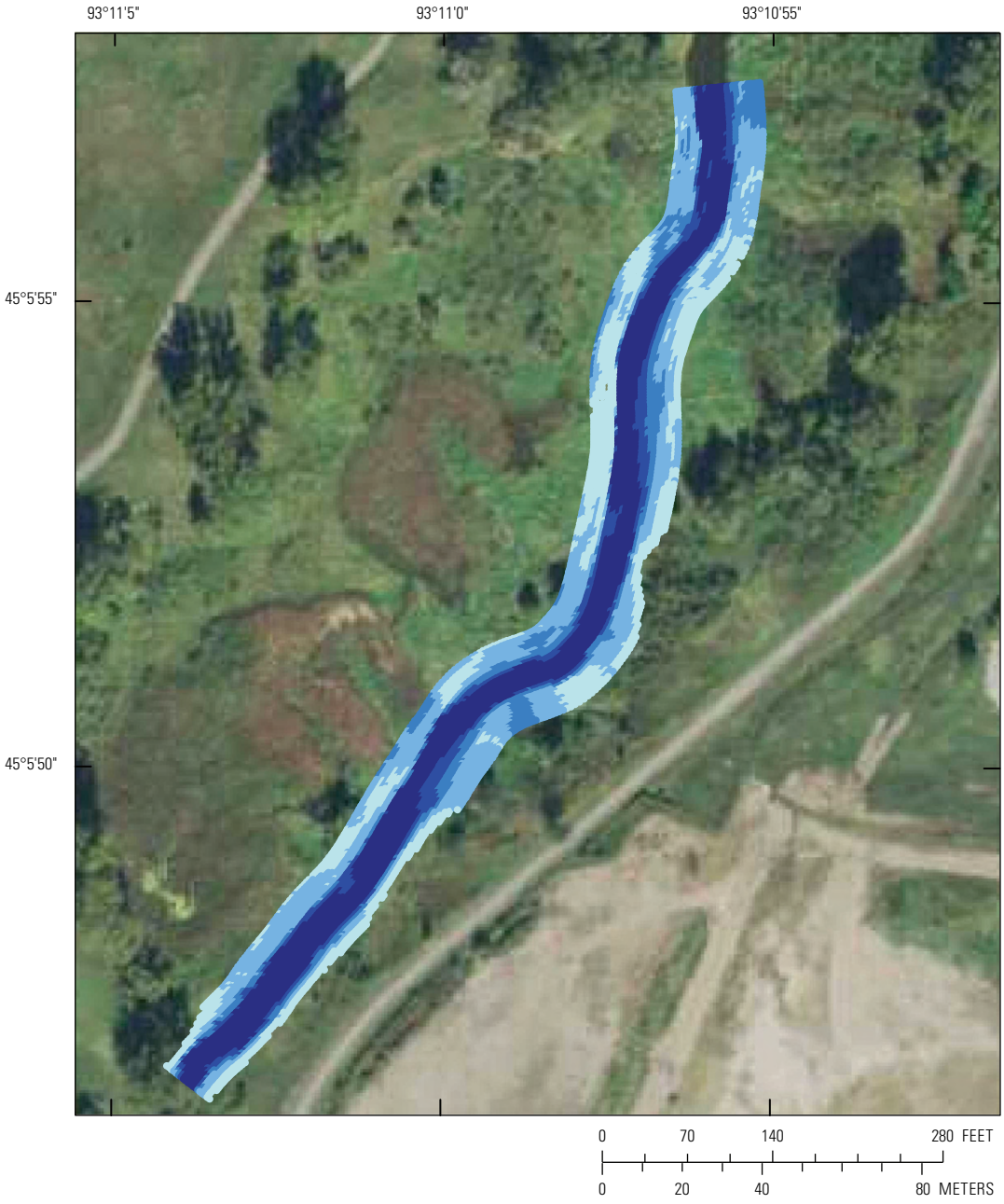

Figure 15.—Continued

F. Modeled water depths post-stream restoration

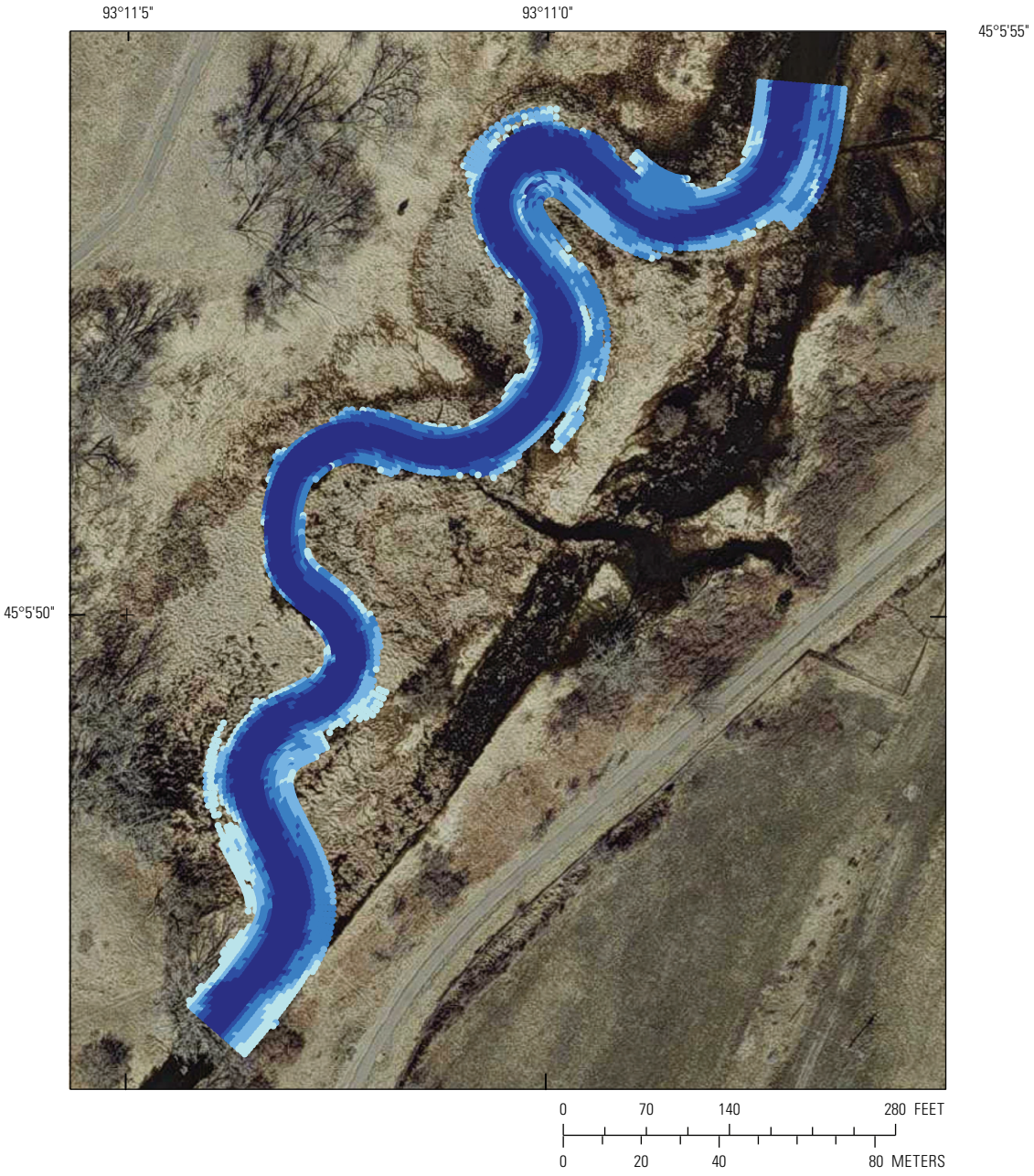

Figure 15.—Continued

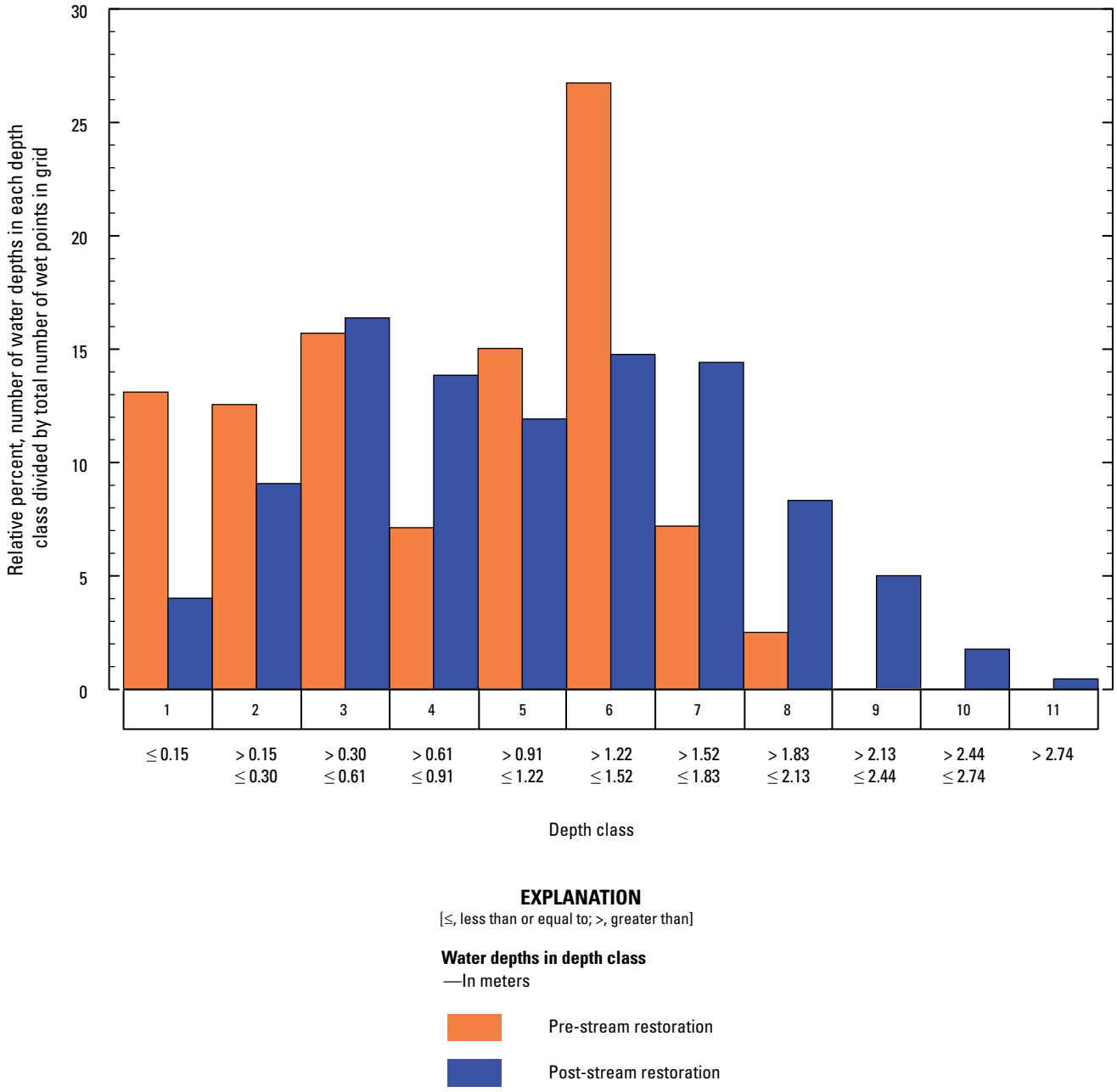

Figure 16. Histogram of pre-stream and post-stream restoration modeled water depths at one streamflow (250 cubic feet per second).

Streamflows of 150, 250, and 400 ft^3/s were selected to illustrate the difference between the pre-stream and post-stream restoration channels (fig. 15). Model simulations indicated that a streamflow of 150 ft^3/s produced two pools in the pre-stream restoration channel and seven pools in the post-stream restoration channel (figs. 15*A* and *B*). Another goal of the stream-restoration design was to increase the complexity of the channel morphology and create more diverse aquatic habitat. The model simulation confirmed an increase in the number of pools in the post-stream restoration channel (seven) compared to the pre-stream restoration channel (two). Since the grid did not extend as far into the floodplain for the post-stream restoration channel as the pre-stream restoration channel, the full extent of water in the floodplain at streamflows of 250 and 400 ft^3/s cannot be accurately depicted in figures 15*D* and *F*.

A. Modeled water velocities pre-stream restoration

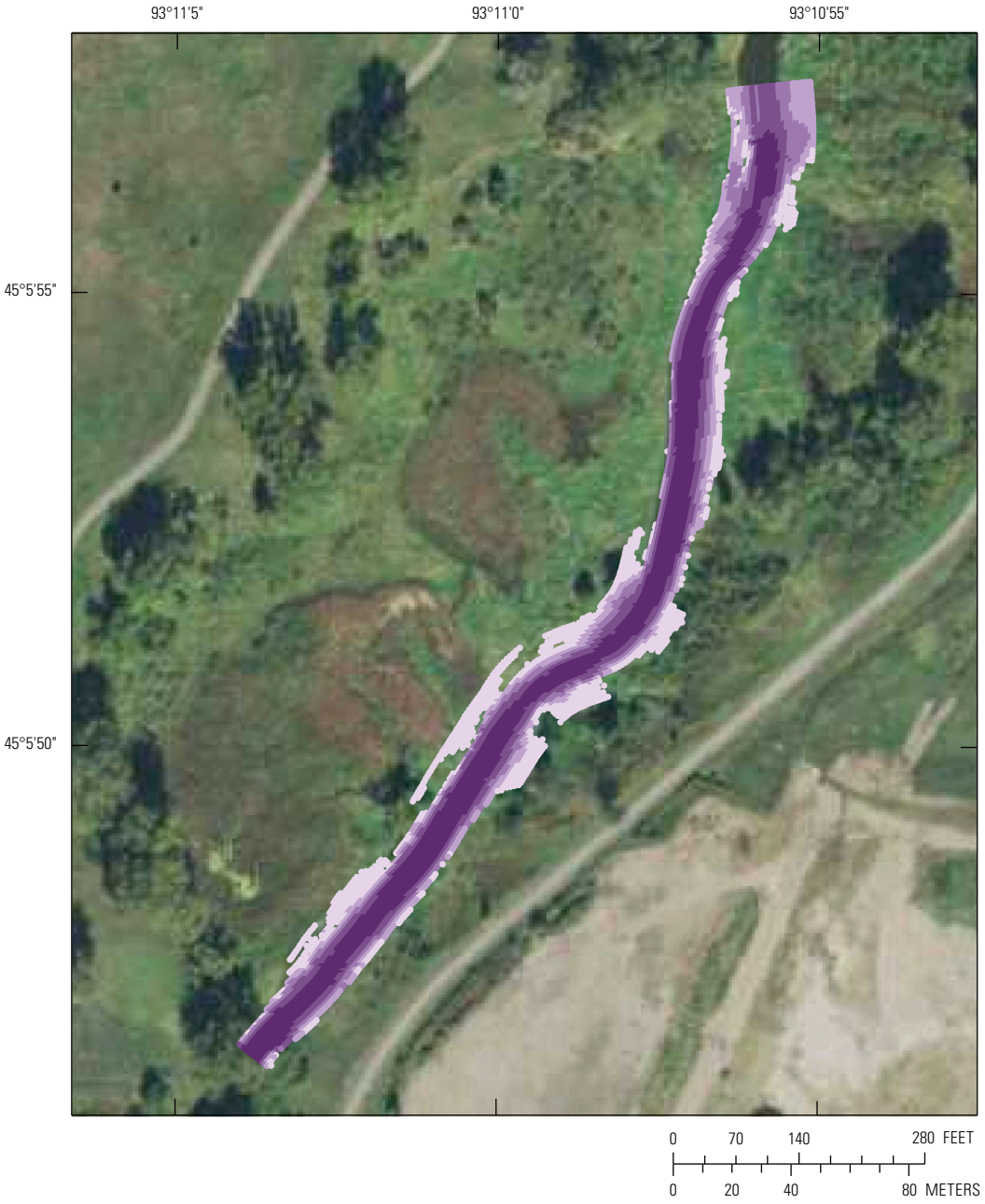

Figure 17. Modeled water velocities, *A*, pre-stream restoration and, *B*, post-stream restoration at one streamflow (250 cubic feet per second).

B. Modeled water velocities post-stream restoration

Figure 17.—Continued

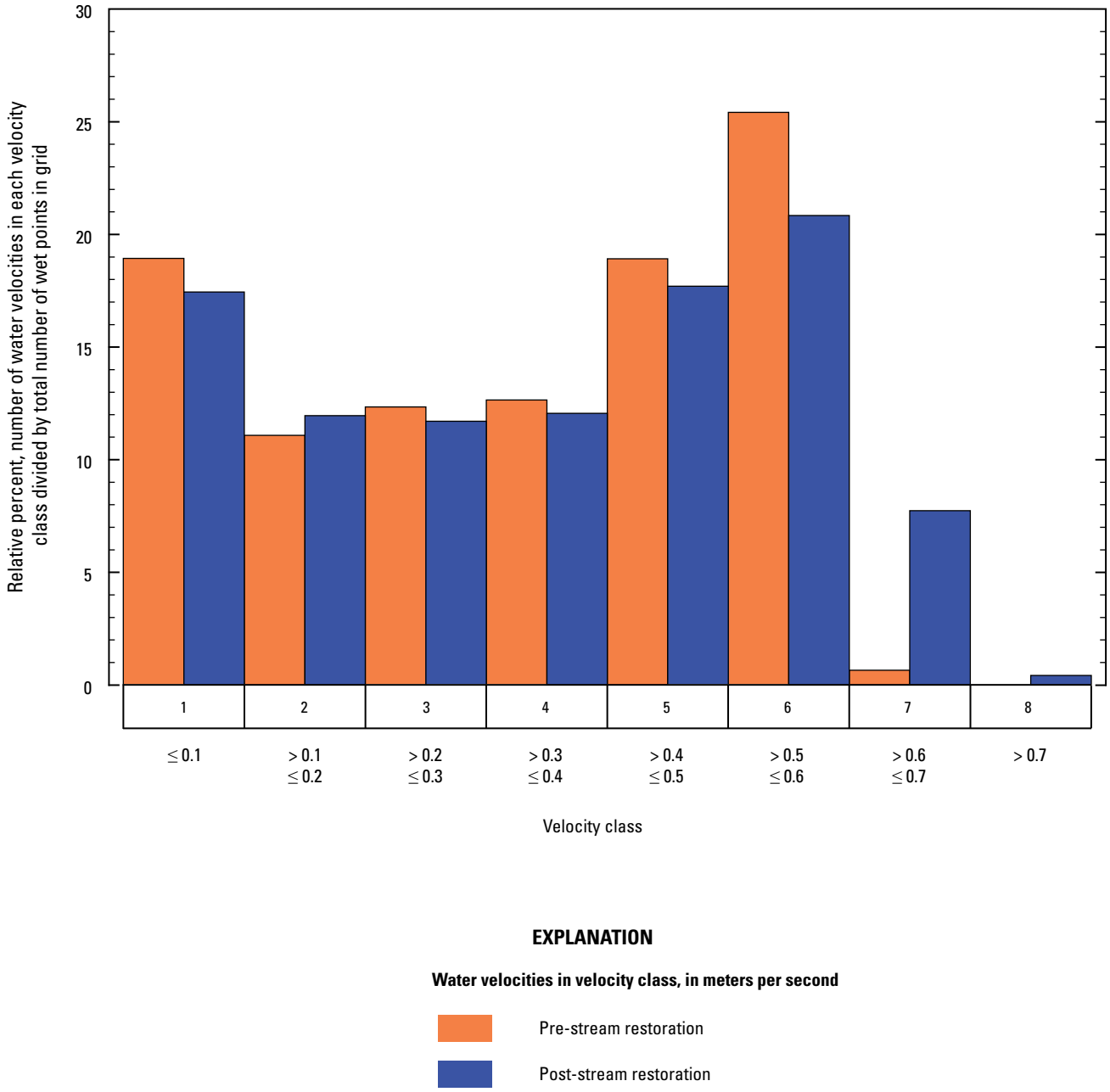

Figure 18. Histogram of pre-stream and post-stream restoration modeled water velocities at one streamflow (250 cubic feet per second).

A streamflow 250 ft^3/s was selected as the bankfull streamflow for the pre-stream restoration channel. This value was within the confidence interval of 226 to 324 ft^3/s for the one-and-a-half-year recurrence interval of 302 ft^3/s (Groten and others, 2022) calculated in PeakFQ (U.S. Geological Survey, 2021b). This streamflow was also used to further compare pre-stream and post-stream restoration channels. The post-stream restoration channel had deeper depths and higher velocities than the pre-stream restoration channel (figs. 15, 16, 17, and 18). The post-stream restoration channel was longer in length and had multiple riffle pools while the pre-stream restoration channel had less variation and was shorter in length. The higher velocities occurred at isolated areas (figs. 17 and 18).

The shear stress was much lower for post-stream restoration channel than the pre-stream restoration channel (fig. 19). Since the post-stream restoration channel has lower shear stress, there will be less potential for degradation and streambank erosion. The post-stream restoration channel can access the floodplain at lower streamflows than the pre-stream restoration channel, so sediment will be more likely to deposit in the floodplain of the post-stream restoration floodplain;

A. Modeled shear stress pre-stream restoration

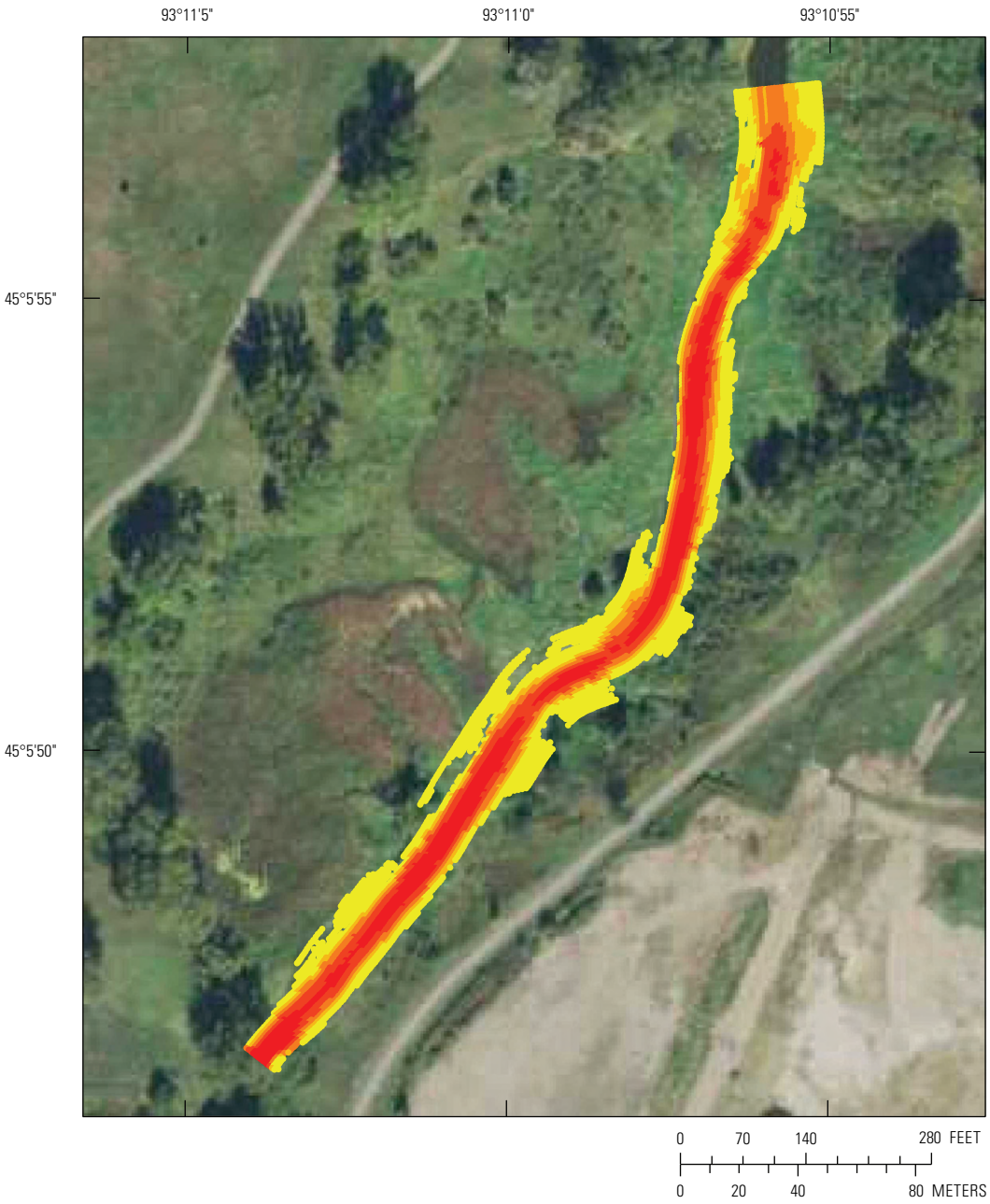

Figure 19. Modeled shear stress, *A*, pre-stream and, *B*, post-stream restoration at one streamflow (250 cubic feet per second).

B. Modeled shear stress post-stream restoration

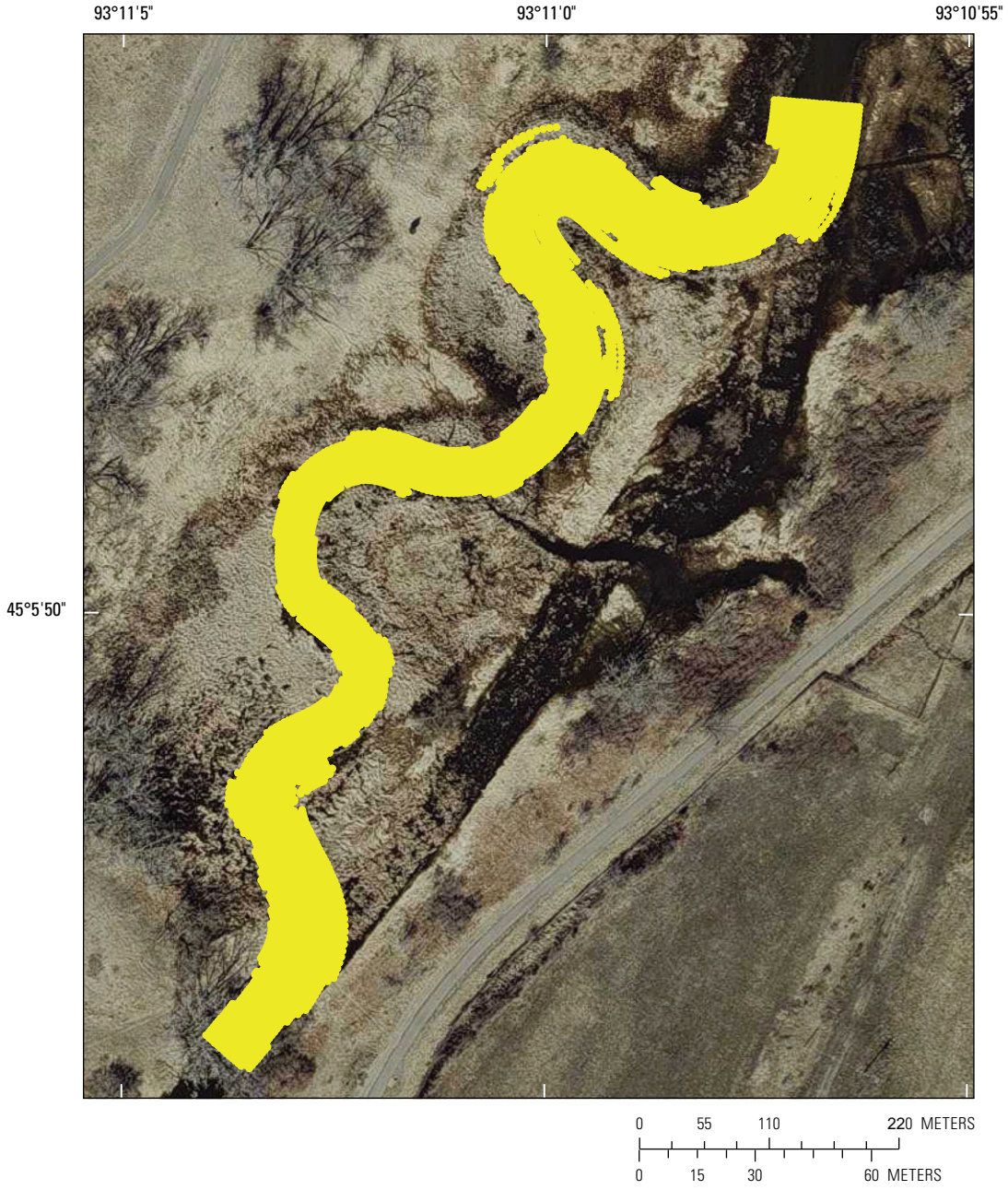

Figure 19.—Continued

however, because of the complexity of sediment transport, the observed sediment transport could also be attributed to other factors or combination of factors not observed, measured, or simulated as part of this study.

Summary and Conclusions

The Rice Creek Watershed District (RCWD) restored two meander sections of Rice Creek in Arden Hills, Minnesota, with goals to reduce water quality impairments, improve aquatic habitat, and reduce associated costs of dredging a sedimentation pond. The RCWD cooperated with the U.S. Geological Survey to establish a 10-year (water years 2010 through 2019) sediment monitoring and flow modeling effort to evaluate the effect of the stream restoration design.

Sampling results were uncertain but indicated there was not a reduction in the post-stream restoration sediment data but an increase because of higher streamflows sampled during the post-stream restoration monitoring period. The negative relation between suspended fines and streamflow was explained by a reduction in the supply of fines with increasing streamflows. The positive relation between suspended sand, bedload, and streamflow was because of those constituents having a functional relation with the hydraulic properties of flow and a consistent supply of sand. Two-dimensional flow modeling simulations indicated the downstream restored section had less shear stress, more pools, and could access the floodplain at a lower streamflow than the original channel.

The results and findings presented in this report are important to the RCWD because it helps inform water-quality criteria for aquatic life and the effect of a stream restoration project. Results and findings support the stream restoration succeeded in reducing shear stress, increasing the number of pools, and promoting access to the floodplain at lower streamflows than the original channel. Overall, the uncertainty in the sampling results indicates the complexity of sediment transport in a river and suggests a need for multisite, multifaceted, multiyear data, and tools to simulate those data for effective evaluations of river restorations.

References Cited

American Society for Testing and Materials, 2000, Standard test methods for determining sediment concentration in water samples—West Conshohocken, Pa., American Society for Testing and Materials International, D3977–97, v. 11.02: Water (Basel), (II): p. 395–400.

Anderson, H.W., 1993, Effects of agricultural and residential land use on ground-water quality, Anoka Sand Plain aquifer, east-central Minnesota: U.S. Geological Survey Water-Resources Investigations Report 93–4074, 62 p. [Also available at https://pubs.er.usgs.gov/publication/wri934074].

Arntson, A.D., Lorenz, D.L., and Stark, J.R., 2004, Estimation of travel times for seven tributaries of the Mississippi River, St. Cloud to Minneapolis, Minnesota, 2003: U.S. Geological Survey Scientific Investigation Report 2004–5192, 17 p.

Childers, D., 1999, Field comparisons of six pressure-difference bedload samplers in high-energy flow: U.S. Geological Survey Water-Resources Investigations Report 92–4068. [Also available at https://doi.org/10.3133/wri924068].

Cooper, W.S., 1935, The history of the Upper Mississippi River in late Wisconsin and post-glacial time: Minnesota Geological Survey Bulletin 26, 116 p.

Davis, B.E., 2005, A guide to the proper selection and use of federally approved sediment and water-quality samplers: U.S. Geological Survey Open-File Report 2005–1087, 20 p. [Also available at https://doi.org/10.3133/ofr20051087].

Dean, D.J., Topping, D.J., Grams, P.E., Walker, A.E., Schmidt, J.C., 2020, Does channel narrowing by floodplain growth necessarily indicate sediment surplus? Lessons from sediment transport analyses in the Green and Colorado Rivers, Canyonlands, Utah: Journal of Geophysical Research: Earth Surface, v. 125, no. 11, p. e2019JF005414.

Dean, D.J., Topping, D.J., Schmidt, J.C., Griffiths, R.E., and Sabol, T.A., 2016, Sediment supply versus local hydraulic controls on sediment transport and storage in a river with large sediment loads: Journal of Geophysical Research. Earth Surface, v. 121, no. 1, p. 82–110.

Domanski, M.M., Straub, T.D., and Landers, M.N., 2015, Surrogate Analysis and Index Developer (SAID) tool (version 1.0, September 2015): U.S. Geological Survey Open-File Report 2015–1177, 38 p., accessed June 26, 2020, at https://doi.org/10.3133/ofr20151177.

Duan, N., 1983, Smearing estimate—A nonparametric retransformation method: Journal of the American Statistical Association, v. 78, no. 383, p. 605–610. [Also available at https://doi.org/10.2307/2288126].

Edwards, T.K., and Glysson, G.D., 1999, Field methods for measurement of fluvial sediment: U.S. Geological Survey Techniques of Water-Resources Investigations, book 3, chap. C2, 89 p. [Also available at https://pubs.usgs.gov/twri/twri3-c2/].

Ellison, C.A., Savage, B.E., and Johnson, G.D., 2014, Suspended-sediment concentrations, loads, total suspended solids, turbidity, and particle-size fractions for selected rivers in Minnesota, 2007 through 2011: U.S. Geological Survey Scientific Investigations Report 2013–5205, 43 p.

Emmons & Olivier Resources, Incorporated, 2008, Middle Rice Creek assessment and stabilization feasibility study: Final report prepared for the Rice Creek Watershed District, 31 p.

Evans, D.J., Johnes, P.J., and Lawrence, D.S., 2004, Physico-chemical controls on phosphorus cycling in two lowland streams. Part 2 – The sediment phase: The Science of the Total Environment, v. 329, no. 1-3, p. 165–182.

Farnham, R.S., 1956, Geology of the Anoka Sand Plain, in Wright, H.E., assoc. ed., The Geological Society of America, Glacial geology, eastern Minnesota: Field Trip No. 3, p. 53–64.

Gray, J.R., and Simões, F.J., 2008, Estimating sediment discharge—Sedimentation engineering–processes, measurements, modeling, and practice: Manual, v. 110, p. 1067–1088.

Groten, J.T., Livdahl, C.T., and DeLong, S.B., 2022, Suspended sediment and bedload data, simple linear regression models, loads, elevation data, and FaSTMECH models for Rice Creek, Minnesota, 2010-2019: U.S. Geological Survey data release, https://doi.org/10.5066/P9SJIY32.

Guy, H.P., 1969, Laboratory theory and methods for sediment analysis: U.S. Geological Survey Techniques of Water Resources Investigations, book 5, chap. C1, 58 p. [Also available at https://pubs.usgs.gov/twri/twri5c1/].

Hamilton, S.K., 2012, Biogeochemical time lags may delay responses of streams to ecological restoration: Freshwater Biology, v. 57, suppl. 1, p. 43–57.

Heidel, S., 1956, The progressive lag of sediment concentration with flood waves: Eos, v. 37, no. 1, p. 56–66.

Helgesen, J.O., and Lindholm, G.F., 1977, Geology and water-supply potential of the Anoka Sand-Plain aquifer, Minnesota: Minnesota Department of Natural Resources, Technical Paper no. 6, 17 p. [Also available at https://www.leg.state.mn.us/docs/pre2003/other/771897.pdf].

Helsel, D.R., Hirsch, R.M., Ryberg, K.R., Archfield, S.A., and Gilroy, E.J., 2020, Statistical methods in water resources: U.S. Geological Survey Techniques and Methods, book 4, chap. A3, 458 p. [Also available at https://doi.org/10.3133/tm4a3].

International River Interface Cooperative [iRIC], 2021, iRIC Software: Changing River Science, accessed February 5, 2020, at https://i-ric.org/en/.

Julien, P.Y., Klaassen, G.J., Brinke, W.B.M.T., and Wilbers, A.W.E., 2002, Case Study—Bed Resistance of Rhine River during 1998 Flood: Journal of Hydraulic Engineering, v. 128, no. 12, p. 1042–1050.

Kleinhans, M., Wilbers, A., and Ten Brinke, W., 2007, Opposite hysteresis of sand and gravel transport upstream and downstream of a bifurcation during a flood in the River Rhine, the Netherlands—Netherlands Journal of Geosciences: Netherlands Journal of Geosciences, v. 86, no. 3, p. 273–285.

Kreiling, R.M., Thoms, M.C., Bartsch, L.A., Richardson, W.B., and Christensen, V.G., 2019, Complex response of sediment phosphorus to land use and management within a river network: Journal of Geophysical Research. Biogeosciences, v. 124, no. 7, p. 1764–1780.

Landers, M.N., and Sturm, T.W., 2013, Hysteresis in suspended sediment to turbidity relations due to changing particle size distributions: Water Resources Research, v. 49, no. 9, p. 5487–5500. [Also available at doi:10.1002/wrcr.20394].

Michalak, A.M., Anderson, E.J., Beletsky, D., Boland, S., Bosch, N.S., Bridgeman, T.B., Chaffin, J.D., Cho, K., Confesor, R., Daloglu, I., DePinto, J.V., Evans, M.A., Fahnenstiel, G.L., He, L., Ho, J.C., Jenkins, L., Johengen, T.H., Kuo, K.C., LaPorte, E., Liu, X., McWilliams, M.R., Moore, M.R., Posselt, D.J., Richards, R.P., Scavia, D., Steiner, A.L., Verhamme, E., Wright, D.M., and Zagorski, M.A., 2013, Record-setting algal bloom in Lake Erie caused by agricultural and meteorological trends consistent with expected future conditions: Proceedings of the National Academy of Sciences of the United States of America, v. 110, no. 16, p. 6448–6452.

Minnesota Department of Natural Resources, 2012, Twin Cities Metro LiDAR 2011: Minnesota Department of Natural Resources web page, accessed April 19, 2017 at https://resources.gisdata.mn.gov/pub/data/elevation/lidar/.

Minnesota Pollution Control Agency, 2014, Rice Creek Watershed District Southwest Urban Lakes: Total Maximum Daily Load Study wq-iw11-19e, 71 p. [also available at https://www.pca.state.mn.us/sites/default/files/wq-iw11-19e.pdf].

Minnesota Pollution Control Agency, 2021, Minnesota's Impaired Waters List: Minnesota Pollution Control Agency web page, accessed February 25, 2021, at https://www.pca.state.mn.gus/water/minnesotas-impaired-waters-list.

National Oceanic and Atmospheric Administration, 2021, Climate at a glance: National Oceanic and Atmospheric Administration web page, accessed on February 8, 2021, at https://www.ncdc.noaa.gov/cag/.

Nelson, J.M., 2016, Fastmech solver manual: International River Interface Cooperative web page, accessed February 5, 2020, at https://i-ric.org/en/download/.

Nelson, J.M., and McDonald, R.R., 1996, Mechanics of modeling of flow and bed evolution in lateral separation eddies: Glen Canyon Environmental Studies Report, 69 p.

Parsons, D.R., Jackson, P.R., Czuba, J.A., Engel, F.L., Rhoads, B.L., Oberg, K.A., Best, J.L., Mueller, D.S., Johnson, K.K., and Riley, J.D., 2013, Velocity Mapping Toolbox (VMT)—A processing and visualization suite for moving-vessel ADCP measurements: Earth Surface Processes and Landforms, v. 38, no. 11, p. 1244–1260.

Porterfield, G., 1972, Computation of fluvial-sediment discharge: U.S. Geological Survey Techniques of Water Resources Investigations, book 3, chap. C3, 65 p. [Also available at https://pubs.usgs.gov/twri/twri3-c3/].

Rice Creek Watershed District, 2017, Rice Creek Watershed District 2017 Annual Report: Rice Creek Watershed District report, 135 p. [Also available at https://www.ricecreek.org.].

Rubin, D.M., Buscombe, D., Wright, S.A., Topping, D., Grams, P., Schmidt, J.C., Hazel Jr, J., Kaplinski, M.A., Tusso, R., 2020, Causes of variability in suspended-sand concentration evaluated using measurements in the Colorado River in Grand Canyon: Journal of Geophysical Research: Earth Surface, v. 125, no. 9, p. e2019JF005226.

Sayers, M., Fahnenstiel, G.L., Shuchman, R.A., and Whitley, M., 2016, Cyanobacteria blooms in three eutrophic basins of the Great Lakes—A comparative analysis using satellite remote sensing: International Journal of Remote Sensing, v. 37, no. 17, p. 4148–4171.

Sharpley, A., Jarvie, H.P., Buda, A., May, L., Spears, B., and Kleinman, P., 2013, Phosphorus legacy—Overcoming the effects of past management practices to mitigate future water quality impairment: Journal of Environmental Quality, v. 42, no. 5, p. 1308–1326.

Shimizu, Y., Giri, S., Yamaguchi, S., and Nelson, J., 2009, Numerical simulation of dune–flat bed transition and stage-discharge relationship with hysteresis effect: Water Resources Research, v. 45, no. 4, p. W04429.

Smith, E.A., Lorenz, D.L., Kessler, E.W., Berg, A.M., and Sanocki, C.A., 2017, Groundwater discharge to the Mississippi River and groundwater balances for the Interstate 94 Corridor surficial aquifer, Clearwater to Elk River, Minnesota, 2012–14: U.S. Geological Survey Scientific Investigations Report 2017–5114, 54 p.

Stone, M. and Mudroch, A., 1989, The effects of particle size, chemistry and mineralogy of river sediments on phosphate adsorption: Environmental Technology Letters, 10, 501–510 p.

Topping, D. J., Grams, P. E., Griffiths, R. E., Dean, D. J., Wright, S. A., and Unema, J. A., 2021, Self-limitation of sand storage in a bedrock-canyon river arising from the interaction of flow and grain size, Journal of Geophysical Research: Earth Surface, 126, e2020JF005565, https://doi.org/10.1029/2020JF005565.

Topping, D.J., Rubin, D.M., Nelson, J.M., Kinzel, P.J., III, and Corson, I.C., 2000a, Colorado River sediment transport—2. Systematic Bed-elevation and grain-size effects of sand supply limitation: Water Resources Research, v. 36, no. 2, p. 543–570.

Topping, D.J., Rubin, D.M., and Vierra, L.E., Jr., 2000b, Colorado River sediment transport—1. Natural sediment supply limitation and the influence of Glen Canyon Dam: Water Resources Research, v. 36, no. 2, p. 515–542.

Topping, D.J., and Wright, S.A., 2016, Long-term continuous acoustical suspended-sediment measurements in rivers—Theory, application, bias, and error: U.S. Geological Survey Professional Paper 1823, 98 p., http://doi.org/10.3133/pp1823.

University of Minnesota, 2021, Minnesota Historical Aerial Photographs Online: University of Minnesota web page, accessed March 22, 2021, at https://apps.lib.umn.edu/mhapo/.

U.S. Department of Agriculture, 2021, Web Soil Survey: U.S. Department of Agriculture web page, accessed March 22, 2021, at https://websoilsurvey.sc.egov.usda.gov/App/HomePage.htm.

U.S. Geological Survey, 2021a, OSW Hydroacoustics: Velocity Mapping Toolbox (VMT): U.S. Geological Survey web page, accessed February 5, 2021, at https://hydroacoustics.usgs.gov/movingboat/VMT/VMT.shtml.

U.S. Geological Survey, 2021b, Peak FQ: Flood frequency analysis software and documentation: U.S. Geological Survey web page, accessed March 24, 2021, at https://water.usgs.gov/software/PeakFQ/.

U.S. Geological Survey, 2021c, USGS water data for the Nation: U.S. Geological Survey National Water Information System database, accessed February 5, 2021, at https://doi.org/10.5066/F7P55KJN.

Warrick, J.A., 2015, Trend analyses with river sediment rating curves: Hydrological Processes, 29(6), 936– 949, at https://doi.org/10.1002/hyp.10198.

Wright, H.E., Jr., 1972a, Physiography of Minnesota, *in* Sims, P.K., and Morey, G.B., eds., 1972, Geology of Minnesota—A centennial volume: Minnesota Geological Survey, p. 561–578. [Also available at https://conservancy.umn.edu/handle/11299/59791].

Wright, H.E., Jr., 1972b, Quaternary history of Minnesota, *in* Sims, P.K., and Morey, G.B., eds., Geology of Minnesota—A centennial volume: Minnesota Geological Survey p. 515–546. [Also available at https://conservancy.umn.edu/handle/11299/59791].

For additional information contact:

Director, Upper Midwest Water Science Center
U.S. Geological Survey
8505 Research Way
Middleton, WI 53562

For additional information, visit:
https://www.usgs.gov/centers/upper-midwest-water-science-center

ISSN 2328-0328 (online)
https://doi.org/10.3133/sir20225004